Tribology International 72 (2014) 65–82

Contents lists available at ScienceDirect

Tribology International

journal homepage: www.elsevier.com/locate/triboint

The role of lubricant feeding conditions on the performance improvement and friction reduction of journal bearings

F.P. Brito [a,b,*], A.S. Miranda [a], J.C.P. Claro [a], J.C. Teixeira [a], L. Costa [c], M. Fillon [d]

[a] Centre for Mechanical and Materials Technologies (CT2M), Mechanical Engineering Department, Universidade do Minho, Campus de Azurém, 4800-058 Guimarães, Portugal
[b] ISEP IPP, Rua Dr. António Bernardino de Almeida 431, 4200-072 Porto, Portugal
[c] Ministry of Energy and Water/DNAAS, Luanda, Angola
[d] Institut Pprime, CNRS, Université de Poitiers, ENSMA, UPR 3346, Dept Génie Mécanique et Systèmes Complexes, SP2MI, 11 Bd Marie & Pierre Curie, BP 30179, 86962 Futuroscope Chasseneuil Cedex, France

ARTICLE INFO

Article history:
Received 1 August 2013
Received in revised form
21 November 2013
Accepted 28 November 2013
Available online 17 December 2013

Keywords:
Journal bearings
Feeding conditions
Thermohydrodynamic model
Groove mixing

ABSTRACT

Most conventional hydrodynamic journal bearing performance tools cannot suitably assess the effect of lubricant feeding conditions on bearing performance, even though these conditions are known to affect important performance parameters such as eccentricity and power loss.

A thermohydrodynamic analysis suitable to deal with realistic feeding conditions has been proposed. Special attention was given to the treatment of phenomena taking place within grooves and their vicinity, as well as to the ruptured film region.

The effect of lubricant feeding pressure and temperature, groove length ratio, width ratio and number (single/twin) on bearing performance has been analyzed for a broad range of conditions. It was found that a careful tuning of the feeding conditions may indeed improve bearing performance.

1. Introduction

The accurate prediction of hydrodynamic journal bearing behavior is far more complex than what their simple geometry might initially suggest. In fact, the simultaneous pressure, flow and heat transfer calculations need to include the treatment of phenomena such as film rupture, dual phase flow, film reformation, forced and free heat convection and conduction, viscous dissipation, inner groove lubricant flow mixing and thermo-elastic distortion. The integrated modeling of these phenomena in a single algorithm displaying acceptable computation times does not seem to be a straightforward task.

The complexity of the problem has frequently led to the use of oversimplified models. Particularly, the incorporation of lubricant feeding conditions was normally made in an oversimplified way in most theoretical approaches or inclusively altogether disregarded. In fact, neglecting the effect of lubricant feeding pressure, feeding temperature or the actual geometry of grooves might explain some of the notable discrepancies found between many theoretical predictions and experimental measurements. These discrepancies seem to be especially acute in the case of twin groove journal bearings. The lack of comprehensive experimental data focusing on these issues might have also contributed for the lack of awareness on the important role which lubricant feeding conditions play on bearing performance.

The inclusion of realistic lubricant feeding conditions in journal bearing analyses might raise some theoretical difficulties, depending on the model used. That is why some models neglect the influence of feeding conditions altogether, while others have used simplified approaches such as the consideration of:

- Full film reformation at the maximum film thickness position or the groove position [1].
- Grooves of infinitesimal width (no circumferential extension) [2,3].
- Grooves of finite width but extending them to the full length of the bush body [4–6].
- Finite size grooves but imposing flow rate or no feeding pressure (ambient) [5].
- Negligible or oversimplified thermal phenomena occurring at the groove region, such as the effect of recirculated hot oil, feeding temperature, reverse flow (oil that re-enters the groove from downstream) or back flow (fresh oil that flows upstream from the groove).

An analysis of the influence of feeding pressure in the performance of twin groove journal bearings through Finite Element

* Corresponding author at: Centre for Mechanical and Materials Technologies (CT2M), Mechanical Engineering Department, Universidade do Minho, Campus de Azurém, 4800-058 Guimarães, Portugal. Tel.: +351 967 381 071.
E-mail address: francisco@dem.uminho.pt (F.P. Brito).

0301-679X/$ - see front matter © 2013 Elsevier Ltd. All rights reserved.
http://dx.doi.org/10.1016/j.triboint.2013.11.016

Nomenclature

A	groove length (axial direction) (m)
b	bush length (axial direction) (m)
c_r	radial clearance (m)
c_{mix}	mixing coefficient used to obtain the leading edge temperature, T_{le}^{+} (dimensionless)
c_p	specific heat at constant pressure (W/kg K)
d	nominal bearing diameter (m)
e_s	thickness of the layer of lubricant adhered to the shaft (Modified Effective Length model) (m)
e_{s0}	fraction of the film height filled with the layer of lubricant adhered to the shaft (Modified Effective Length model) (dimensionless)
$\overline{EL}$	effective length ratio (fraction of the bearing length filled with liquid streamers for a given circumferential coordinate) (dimensionless)
$\overline{EL}_m$	modified effective length ratio (same as EL but corrected for the modified effective length model) (dimensionless)
h	local film thickness (m)
h_{min}	minimum film thickness (m)
K	thermal conductivity (W/m K)
N	shaft rotational speed (rpm)
P	hydrodynamic pressure within the film (relative to ambient pressure) (Pa)
P_f	lubricant feeding pressure (relative to ambient pressure) (Pa)
q	heat transfer rate (W)
Q_f	lubricant feeding flow rate (l/min)
r	radial coordinate (bush body domain)/nominal bearing radius (m)
T_{amb}	ambient temperature – the average temperature of the bearing system environment (°C)
T_b	bush body temperature field variable (°C)
T_f	lubricant feeding temperature (°C)
T_{max}	maximum bush temperature (°C)
u	fluid velocity field variable (m/s)
U	tangential velocity of the shaft surface (m/s)
W	applied load/load carrying capacity (N)
W_s	specific load (the load divided by the projected area of the bush ($b \bullet d$)) (Pa)
w	groove width (circumferential direction) (m)
x	circumferential coordinate of the unwrapped geometry (m)
y	radial coordinate (fluid domain) (m)
z	axial coordinate (m)

Greek symbols

α	circumferential coordinate – angle measured from the centre of the $+90^{\circ}$ groove (deg)
ε	eccentricity ratio (dimensionless)
ϕ	attitude angle (deg)
θ'	liquid fraction (volumetric) (dimensionless)
μ	dynamic viscosity (Pa s)
ρ	density (kg/m^3)

Subscripts

axial	corresponding to the lateral edges of the groove or to the lubricant crossing them
bkf	corresponding to back flow (oil leaving the groove through the trailing edge, in the upstream direction)
eq	corresponding to the equivalent property of the flowing mixture (gaseous + liquid)
g	corresponding to the gaseous portion of the flowing mixture
f	corresponding to feeding conditions
gr	corresponding to a groove
is	corresponding to the inlet section of a bearing land (the whole bush section at the coordinate of the leading edge of the groove)
H	corresponding to convective heat transfer inside the groove regions
l	corresponding to the liquid portion (lubricant) of the flowing mixture
le	corresponding to the leading edge of a groove (downstream edge)
out	corresponding to outlet flow rate leaking from the bearing through its edges
rvf	corresponding to reverse flow (oil entering the leading edge of the groove coming from downstream)
te	corresponding to the trailing edge of a groove (upstream edge)

Abbreviations

CFD	Computational Fluid Dynamics
EL	Effective Length model
EL_m	Modified Effective Length model
GRE	Generalized Reynolds Equation
RPM	Revolutions Per Minute
TEHD	Thermoelastohydrodynamic
THD	Thermohydrodynamic

Methods was performed by Knight et al. [7]. A 1D energy equation was used and the axial pressure profile described through second order polynomials. It was shown that the feeding pressure affects the maximum temperature decreasing it, especially at low Sommerfeld numbers. The increase in feeding pressure was found to increase significantly the flow rate and slightly the power loss.

A series of theoretical and experimental studies on high speed twin groove journal bearings were carried out by Gethin and El-Deihi [8,9] in order to assess the influence of the position of the two diametrically opposed axial grooves relatively to the load direction. In this last work a more rigorous THD approach was used, in comparison to the former works. Viscosity and temperature were allowed to vary along the thickness and heat conduction through the solid bodies was considered. The shaft temperature was imposed as being equal to the mean film temperature, while at the leading edge of the groove the inlet temperature was calculated through a heat balance. The use of such a groove mixing model proved to be determinant for the improvement of the results. With this new model a much better agreement with experiment was found for the temperature profile. However, huge differences between theory and experiment continued to be detected in flow rate.

Attention to film reformation and the use of mass conserving algorithms for treating feeding conditions was highlighted by Dowson et al. [10]. A thorough theoretical and experimental assessment of the influence of lubricant feeding conditions on the performance of circular journal bearings with several groove configurations was made by Claro and Miranda [11], including twin axial groove journal

bearings. Although this analysis was based on an isoviscous approach, a mass conservative algorithm proposed by [12] was used considering the actual dimensions of the grooves. Later [13], this approach was extended to take into account thermal effects, and validated with experimental evidence [14] on the influence of lubricant feeding conditions on the performance of single groove journal bearings. It was shown that often neglected parameters such as the real value of the feeding pressure and the actual groove geometry and location can significantly influence bearing performance.

Ma and Taylor [15–17] used a theoretical approach based on the separation model and also carried out some experimental work in order to study the influence of feeding temperature and feeding pressure on the performance of twin groove elliptical bearings. It was found that the increase of feeding temperature yielded significantly higher values of the maximum temperature and flow rate and significantly lower values of power loss. On the other hand, increasing feeding pressure caused an important increase in flow rate, and moderate decreases in maximum bush temperature and power loss.

Vijayaraghavan [18] analyzed the effect of lubricant feeding starvation on the THD performance of a journal bearing with a single axial groove. A previously developed model [19] was used, leading to the conclusion that a judicious selection of the groove location could reduce substantially the flow rate and the power loss without a deleterious effect in load carrying capacity.

An analysis of the influence of oil inlet conditions on the THD performance of the fully circumferentially grooved journal bearings was performed by Keogh and Khonsari [20]. A simplified axial averaging technique was used, that enabled the groove pressure and the entry temperature to the lubricant film to be explicitly incorporated into the lubricant energy equation and highlighted that the mixing effect must be always taken into account.

As a final remark, it may be concluded the experimental works focusing on twin groove journal bearings were found to be scarce or incomplete, namely in what concerns to the influence of feeding conditions and how these conditions may be tuned in order to optimize bearing performance and reduce power loss.

Effectively, Tonnesen and Hansen [21], as well as Lund and Tonnesen [22] carried out a good experimental work on these bearings, but with fixed feeding conditions. The same can be said of the work by Fitzgerald and Neal [23], which also lacks some other important data such as shaft eccentricity conditions. Gethin and El-Deihi [8,9] presented very interesting experimental results of the behavior of a twin groove journal bearing under several load angles. Unfortunately the speeds tested were normally too high to consider a laminar regime. Finally, Ma and Taylor [16] presented experimental results for this bearing type but omitted the main lubricant properties. Furthermore, the test bearing possessed unusually large grooves, spanning 55° each. It seemed that an experimental work testing a wide range of lubricant feeding conditions still needed to be done.

Recently the authors have published some works to address this lack of information. They assessed the influence of feeding temperature and feeding pressure on the performance of a 100 mm twin axial groove bearing [24] and it was found that increasing feeding pressure leads to a significant rise in oil flow rate but has little effect on the maximum temperature and power-loss, except for the case of the lightly loaded bearing. Shaft temperature was found to be close to the bearing maximum temperature for low applied loads, being significantly smaller than this value for high loads. The mean shaft temperature was found to be significantly higher than the outlet.

Also the role of each groove on the behavior of a twin axial groove 50 mm journal bearing was assessed [25]. As a novelty, they carried out the measurement of the flow rate in each groove and discovered that indeed groove flow rate information is vital to fully understand bearing behavior. It was found that the cooling effect of the downstream groove is small for low eccentricities, becoming more relevant as eccentricity increases. The opposite phenomenon occurs at the upstream groove. Under high load/low feeding pressure negative flow rate at the upstream groove was detected dramatically affecting the bearing performance. Increasing feeding pressure yielded to a decrease in shaft eccentricity along with a temperature decrease, especially for high loads.

Another work was done with the same rig but focusing on the role of feeding temperature [26]. It was found that the increase of T_f has an effect in bearing performance which is analogous in many ways to the effect of the increase in eccentricity: increase in lubricant flow rate (especially in the low eccentricity range), in outlet temperature and in maximum bush temperature (T_{max}). Nevertheless, the latter increase was lower than the corresponding increase in T_f.

The authors carried out an original comparison on the performance of a journal bearing with a single ($+90°$ to the load line) and a twin ($\pm 90°$) axial groove configuration [27]. It was found that under heavy loaded operation the twin groove configuration might sometimes deteriorate the bearing performance when compared with the single groove arrangement, namely due to uneven lubricant feed through each groove. It was concluded that the knowledge of the feed flow rates through each groove can be used to improve bearing performance under specific regimes by implementing groove deactivation or flow balancing strategies.

Recently, they assessed the influence of load direction on the behavior of a twin axial groove bearing [28]. The general trend found was that increasing groove angle tends to decrease the flow rate at the upstream groove and to increase the flow rate at the downstream groove. Hot oil reflux (negative flow rate) may occurs on both grooves (although, naturally, never simultaneously) under some conditions. The flow rate trends were mainly explained by the proximity to the pressure build-up zones and their locations relative to each groove.

Realistic feeding conditions such as the actual groove geometry and location, lubricant feeding pressure and lubricant feeding temperature, have been often neglected or oversimplified in most theoretical models. This has limited the analysis of important related phenomena such as the occurrence of reverse-flow at the inlet region, lubricant back-flow to the region which is located upstream of grooves, the mixing at the grooves, the inlet temperature profile, the occurrence of film rupture and reformation and the feeding flow rate.

The present work tries to address some of these concerns by presenting a model for the analysis of hydrodynamic Journal bearings which is suitable for assessing the aforementioned phenomena. It seems that an effort should be put on the development of an extensively validated model which may enable a better understanding of some of the mechanisms which can significantly affect the performance of common hydrodynamic journal bearings, and are still not thoroughly studied or satisfactorily dominated.

The decision of focusing the present study on twin groove journal bearings was based not only on the fact that this bearing geometry has received much less attention than single groove cases, but also because more acute theoretical performance prediction discrepancies have been observed for this bearing geometry. In fact, most theoretical models do not conveniently represent the temperature field in the ruptured film region and in the vicinity of grooves, and largely overestimate flow rate. Moreover, there are specific issues related to twin groove configuration, such as flow rate partition between the grooves and the occurrence of negative flow rate at one of the grooves, which are still not sufficiently studied and deserve further attention.

A Thermohydrodynamic (THD) approach was implemented. It was based on the simultaneous solution of the Generalized

Reynolds Equation and the Energy Equation within the fluid domain and the Laplace equation within the bush body domain. Care was taken in order to realistically incorporate lubricant feeding conditions into the analysis: the real dimensions of the grooves were considered in pressure and flow calculations, mass and energy conserving algorithms were deployed. Models for the ruptured film region and the lubricant mixing at the grooves were derived. A simplified thermo-elastic model was implemented. Suitable boundary conditions were pursued. After describing the model a careful validation of the theoretical model with comparisons between its results and experimental data is presented. Finally, an extensive parametric study to assess the influence of lubricant feeding conditions such as feeding pressure and temperature, groove length and groove width ratio and number of grooves (single/twin) on bearing performance is carried out and discussed.

2. Theoretical model

The theoretical model for the analysis of the steady state performance of journal bearings and especially adapted for the assessment of lubricant feed conditions is presented in continuation. It is an evolution of previous isoviscous [11] and thermo-hydrodynamic (THD) [13] models proposed by the group. Details concerning more specific issues such as the variable transformations or the expressions used for the calculation of velocity profiles, flow rates and heat transfer rates have been detailed in [29], and so a more condensed description is made here. The model incorporates the full Thermohydrodynamic (THD) analysis and treats realistically the lubricant feeding conditions, namely taking into consideration the lubricant feeding pressure, the feeding temperature and the actual groove dimensions.

Based on input data such as the physical properties of the lubricant and bearing components, the operating conditions, the geometric configuration of the bearing and the lubricant feeding conditions, the model is expected to provide the main performance parameters relevant to bearing design and performance analysis, such as the hydrodynamic pressure and temperature profiles, oil flow rate, minimum film thickness, eccentricity, attitude angle, shaft torque, and power loss.

An outline of the bearing geometry, with all the major geometric characteristics identified, is presented in Fig. 1.

The unwrapped bearing gap geometry, with the corresponding axis system can be observed in dimensional and non-dimensional normalized form in Fig. 2, respectively, under the reasonable assumption that bearing curvature and inertial effects may be neglected.

2.1. Pressure and velocity fields

Widely accepted assumptions have been made regarding the pressure and flow field calculation. They include the thin film approximation, where pressure does not vary across the film thickness (not valid within groove regions); flow is in the laminar regime, with fluid inertia and gravity effects being negligible when compared with viscous effects; steady state regime; the fluid is incompressible and Newtonian, with lubricant viscosity depending solely on temperature; the effect of the bearing curvature is negligible (clearance is much smaller than the bearing radius); there is no contact between surfaces and the effect of surface roughness is negligible (hydraulically smooth surface in the fully hydrodynamic regime); thermal expansion suffered by the components is uniform and based on their average temperature (only their diameter is affected – i.e. a differential thermal expansion approach).

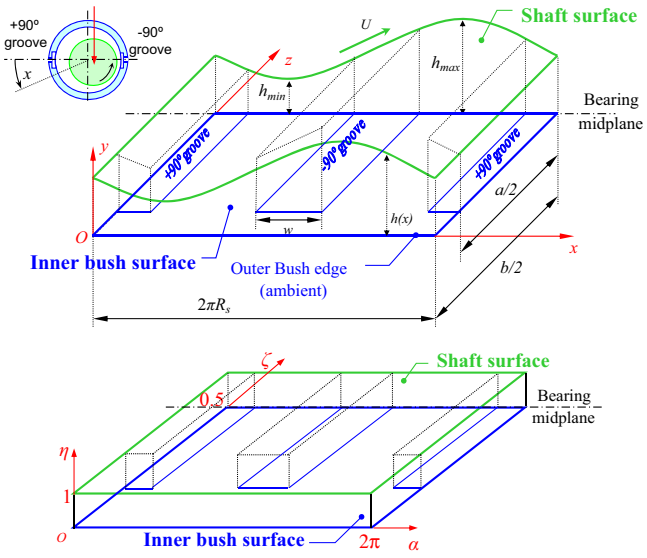

Fig. 2. Unwrapped dimensional and non-dimensional (normalized) fluid domain.

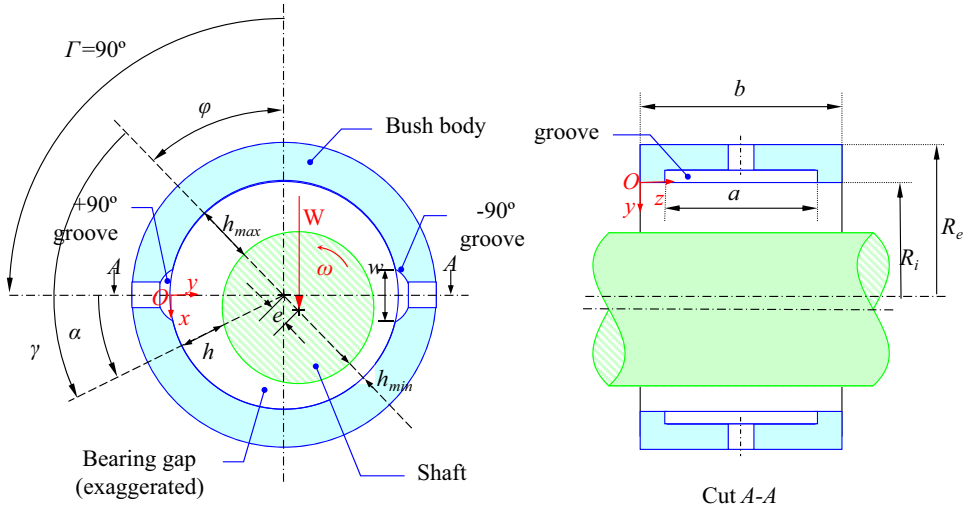

Fig. 1. Outline of the bearing geometry.

Table 1
Geometric characteristics, operating and feeding conditions used in the analysis.

Geometric characteristics	Units	**Default value**/range
Inner bush diameter (nominal) (d)	mm	**100**
Outer bush diameter (D)	mm	**200**
Bush width/diameter ratio (b/d)		0.8
Groove number		1; 2
Groove angle with load line		$+90^\circ$; $\pm$**90**$^\circ$
Groove length/bush length ratio (a/b)		0.30; 0.6; **0.875**
Groove width/diam. ratio (w/d)		**0.18**; 0.16
Bearing radial clearance (at 20 ºC) (C_r)	μm	**75**
Operating and feeding conditions		
Rotational speed (N)	krpm	1; **3** ; 5
Specific load range (approx.) (W_s)	MPa	0.1–10
Oil feeding pressure (P_f)	kPa	0; 50; **100**; 200; 300
Oil feeding temperature (T_f)	°C	30; **40**; 50; 60

Table 2
Lubricant properties used in the analysis.

Lubricant properties		Value
T1	°C	40
T2	°C	70
Dynamic viscosity @ T1 (μ_{T1})	Pa s	0.0293
Dynamic viscosity @ T2 (μ_{T2})	Pa s	0.0111
Specific heat (C_p)	J/kg K	2000
Density (ρ)	kg/m^3	870
Thermal conductivity (k)	W/m K	0.13

The hydrodynamic pressure field, $P(x,z)$ is governed by the Generalized Reynolds Equation (GRE), which is derived from a flow balance [30]:

$$\underbrace{\frac{\partial}{\partial x}\left[\rho_l F_2 \frac{\partial P}{\partial x}\right]}_{\text{Due to circumferential Poiseulle flow (pressure driven)}} + \underbrace{\frac{\partial}{\partial z}\left[\rho_l F_2 \frac{\partial P}{\partial z}\right]}_{\text{Due to axial Poiseulle flow (pressure driven)}} = \underbrace{U\frac{\partial}{\partial x}[\rho_l h F_3]}_{\text{Due to circumferential Couette flow (drag driven)}} \quad (1)$$

with the viscosity integrals, which account for cross-film viscosity variation, being defined as follows:

$$F_0 = \int_0^h \frac{1}{\mu_l} dy \quad ; \quad F_1 = \int_0^h \frac{y}{\mu_l} dy \quad ;$$
$$F_2 = \int_0^h \frac{y}{\mu_l}\left(y - \frac{F_1}{F_0}\right) dy \quad ; \quad F_3 = 1 - \frac{F_1}{hF_0} \quad (2)$$

The viscosity–temperature relationship is ruled by the McCoull and Whalther expression [30] with the coefficients of the expression being deduced based on two viscosity values at two different temperatures (see Table 2). The standard solution of Eq. (1) is only suitable within the full film region, where pressure is greater than ambient ($P>0$). The lubricant is not able to withstand low pressures (e.g. sub-ambient), separating in a series of streamlets separated by gaseous cavities and remaining at uniform pressure (in this work considered as ambient). So, a suitable algorithm must be used in order to locate the ruptured film region borders and then provide a special treatment to this region. The rupture boundary may be obtained with the so-called Reynolds condition, where pressure and pressure gradients in the direction of bearing rotation are considered to be zero. This condition ensures flow continuity and it is widely accepted in bearing modeling.

Concerning the film reformation boundary condition, some authors make the simplifying assumption of considering it to occur at the position of maximum film thickness or at the circumferential coordinate of grooves, which are considered to have negligible thickness and to span the whole bearing length. However, this condition is rather an imposition of the location of film reformation rather than a method for estimating it. This is highly unsuitable when considering realistic feeding conditions as is the aim of the present work.

In reality, film reformation will occur once locally the bearing gap is filled with lubricant (at the circumferential location where the remaining, recirculated, flow volume is enough to fill the gap), and this can be computed based on knowledge over the flow patterns and flow continuity. In fact, the GRE is basically an equation which computes flow continuity accounting for the various flow components existing within the bearing gap. Considering the aforementioned simplifying assumptions, these flows will be reduced to pressure-driven flow (Poiseuille) and the drag-driven flow (Couette). Within the ruptured film region the pressure is normally considered to be ambient and thus the flow will be purely drag-driven. In this way, mass flow continuity may be easily computed and film reformation boundary located. It is therefore possible to change the character of the GRE in the ruptured film region adapting it to a mass conserving equation which is valid throughout the whole bearing domain. Such was accomplished with the algorithm proposed by Elrod [12]. It is based on the mass balance performed to the Couette and Poiseuille flows crossing a finite control volume surrounding each computational node. The computation of Poiseuille and Couette flows will be performed at the full film region while Couette flow and liquid fraction will be accounted for at the ruptured film region. A substitution variable including a switch function which is either 0 or 1 whether the film is ruptured ($P=0$) or full width ($P>0$) is used for this. The result is a mass conservative, finite difference version of the Reynolds equation, valid throughout the whole domain and solved iteratively through the Gauss–Seidel method, and with the switch function being updated at each iteration.

The present work uses this algorithm, as adapted to THD by Costa et al. [13]. An advantage of this method is that it automatically provides the mass flow rates of lubricant crossing all faces of each computation cell and the corresponding local liquid fraction at the ruptured film region. This is very suitable for computing flow rates in places such as groove edges (something vital for analyzing feed conditions) and for use in ruptured film region thermal models based on effective length concepts such as those described in [4].

The velocity field must also be computed, as it affects the convective and the dissipative terms of the energy equation. The expressions for the circumferential and axial components of the velocity are the sum of the Poiseuille and Couette components for variable viscosity [30]:

$$\begin{cases} u_x = \frac{\partial p}{\partial x}\left(F_4 - \frac{F_1 F_5}{F_0}\right) + U\frac{F_5}{F_0} \\ u_z = \frac{\partial p}{\partial z}\left(F_4 - \frac{F_1 F_5}{F_0}\right) \end{cases} \text{ with } \begin{cases} F_4 = \int_0^y \frac{\lambda}{\mu_l} d\lambda \\ F_5 = \int_0^y \frac{1}{\mu_l} d\lambda \end{cases} \quad (3)$$

being λ a dummy variable of y. The radial velocity u_y is obtained from the solution of the flow continuity equation computed solely for the liquid portion of the flow, which must be affected by the local liquid fraction, θ':

$$\frac{\partial(\theta' u_x)}{\partial x} + \frac{\partial(\theta' u_z u_y)}{\partial y} + \frac{\partial(\theta' u_z)}{\partial z} = 0 \quad (4)$$

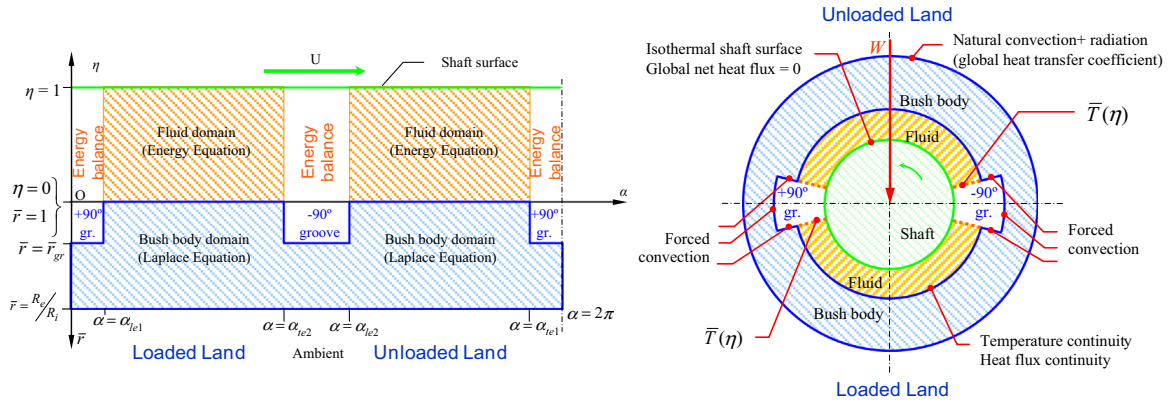

Fig. 3. Outline of the calculation domains and boundary conditions used in the thermal model.

2.2. Thermal model

The thermal problem is coupled with the flow problem in the sense that viscous dissipation depends on velocity gradients, while the pressure and velocity fields will depend on viscosity, which is temperature dependent.

There are basically three calculation domains, as depicted in Fig. 3: the Fluid Domain, where the Energy equation is solved; the Bush Body domain, where the Laplace equation, which governs conductive heat transfer, is solved. Finally there are the groove regions, where the Reynolds equation is not applicable (thin film condition is not valid). In this latter domain only mass and energy balances are performed. The various domain interfaces are dealt with specific boundary conditions, as depicted in Fig. 3.

Some of the simplifying assumptions include: neglecting the axial temperature gradients (calculations are performed in the mid-plane only), with this assumption being backed by both experimental [23,31,32] and theoretical evidence [3,33] for usual operating conditions and lengthy grooves (nevertheless, specific modeling is proposed in the present work to compensate for axial gradients, especially for the case of small grooves); the circumferential and axial diffusive terms may be neglected when compared with the corresponding convective terms (high Peclet number) [30], which leads to purely radial conductive heat transfer; only dissipative terms based on transverse gradients are relevant [30]; the bearing is perfectly aligned, i.e. axial symmetry is assumed.

2.2.1. Fluid domain

The aforementioned assumptions lead to the following simplified form of the energy equation at the mid-plane of the bearing [30]:

$$\underbrace{(\rho c_p)_{eq}\left[u_x\frac{\partial T}{\partial x}+u_y\frac{\partial T}{\partial y}\right]}_{\text{convective term (convection)}} = \underbrace{K_{eq}\frac{\partial^2 T}{\partial y^2}}_{\text{diffusive term (conduction)}} + \underbrace{\mu_{eq}\left(\frac{\partial u_x}{\partial y}\right)^2}_{\text{dissipative term}} \quad \text{(heat generation)} \tag{5}$$

$(\rho c_p)_{eq}$ and K_{eq} are the properties (density, specific heat and thermal conductivity) of the lubricant or the equivalent properties or the lubricant streamers plus gaseous cavities at the ruptured film region. These will depend on the specific modeling of the ruptured film region. It is common to use the "Effective Length" concept to model the ruptured film region [4]. In fact, if both the lubricant streamers and the gaseous cavities are attached to the bush and shaft surfaces and considering heat transfer to occur radially and in parallel through liquid and gaseous streamers, it may be proved that the equivalent physical properties of the liquid plus gas mixture will be an average of the liquid and gas properties weighted by their corresponding fraction in the mixture, with a particularity found by the authors in which the density and specific heat should be treated as a group, as seen in (1). The effective fraction of the bearing length which is filled with liquid lubricant is therefore called the effective length of lubricant, $\overline{EL}$, easily computed by integrating the fluid fraction along the relevant section. The equivalent properties will therefore be the following:

$$\begin{cases} (\rho\, C_p)_{eq} = \overline{EL}\rho_l c_{pl} + (1-\overline{EL})\rho_g C_{pg} \\ K_{eq} = \overline{EL}K_l + (1-\overline{EL})K_g \\ \mu_{eq} = \overline{EL}\mu_l + (1-\overline{EL})\mu_g \end{cases} \tag{6}$$

It is important to acknowledge that these equivalent properties (namely the equivalent viscosity) will only be valid for the thermal calculations (they have been derived based on the energy equation). The properties used for the pressure and flow calculations will be solely based on those of the liquid portion of the flow.

There is experimental evidence that in the ruptured film region not all the lubricant flows along streamers that are attached to both the shaft and bush surfaces. In reality, a portion of it is attached solely to the shaft surface forming an adhered layer to this surface [34,35]. This will affect heat transfer since no velocity gradients (and therefore no heat dissipation) will be present for that portion of the lubricant. Some authors have taken this phenomenon into account [4], although within the scope of a simplified model.

The following expressions for the equivalent properties for thermal calculations, which will vary according to the radial position in the film (whether in the layer region or the streamer-only region) have been derived (see outline of this modeling in Fig. 4):

Streamer – only region $(0 \le \eta < 1-\bar{e}_s(\alpha))$

$$\begin{cases} (\rho\, C_p)_{eq} = \overline{EL}_m\rho_l c_{pl} + (1-\overline{EL}_m)\rho_g C_{pg} \\ K_{eq} = \overline{EL}_m K_l + (1-\overline{EL}_m)K_g \\ \mu_{eq} = \overline{EL}_m\mu_l + (1-\overline{EL}_m)\mu_g \end{cases}$$

Layer region $(1-\bar{e}_s(\alpha) \le \eta \le 1)$

$$\begin{cases} (\rho C_p)_{eq} = \rho_l c_{pl} \\ K_{eq} = K_l \\ \mu_{eq} = \overline{EL}_m\mu_l \end{cases} \tag{7}$$

With $\overline{EL}_m$ being the corrected Effective Length of lubricant, which corrects $\overline{EL}$ in order to reflect the portion of lubricant which has been taken out of streamer flow (Couette flow) and allocated to the shaft adhered layer (uniform flow). $e_s(a)$ Is the fraction of the bearing gap occupied by the lubricant layer at a given circumferential position α, calculated by continuity from its initial value at the rupture front, e_{s0}, and the variation of the local film height, $e_s(a)$:

$$\overline{EL}_m = \frac{\overline{EL}-2\bar{e}_s(\alpha)}{1-2\bar{e}_s(\alpha)}, \quad \bar{e}_s(\alpha) = \bar{e}_{s0}\frac{\bar{h}(\alpha_{rupt})}{\bar{h}(\alpha)} \tag{8}$$

It may be easily deduced that if all the lubricant will flow adhered to the shaft with no streamers present $\overline{EL}_m$, the fraction of the bearing gap occupied by the lubricant layer will be at the best 0.5 (the linear profile of the Couette flow of the streamers will be converted into a uniform velocity profile possessing the speed of the shaft) and no heat dissipation will occur. Again, the existence of this shaft-adhered layer has been considered only for the thermal model. The computation of cell flow rates which is the basis for the pressure field calculation relies on the assumption that in the ruptured film region the lubricant flows solely along streamers attached both to the bush and the shaft surfaces.

The energy equation is solved through a method proposed by Boncompain et al. [3], which consists in solving the energy equation as an initial value problem in the circumferential direction. This may be done as long as the circumferential velocity component is positive. However, if a region with negative speed exists, then this solution scheme may still be applied using the domain separation iterative approach, where calculations are performed successively in the two separate speed domains (positive and negative) as an initial value problem and in the direction of the flow. The results of one domain will be used as a boundary/initial conditions for the other one.

2.2.2. Bush body domain

The conductive heat transfer across the bush body is solved through the Laplace Equation for cylindrical coordinates [30]:

$$\frac{\partial^2 T_b}{\partial r^2}+\frac{1}{r}\frac{\partial T_b}{\partial r}+\frac{1}{r^2}\frac{\partial^2 T_b}{\partial \alpha^2}=0 \tag{9}$$

This equation is elliptical and may be solved iteratively through the successive over-relaxation method. Once again, no axial flux is considered to occur, so the terms in the z direction have vanished.

2.2.3. Groove regions

A suitable thermal modeling of the phenomena taking place within groove regions and their surroundings is vital when analyzing the role of feeding conditions. However, within groove regions (recall Fig. 3) the thin film assumption ($c_r \ll r$) which is the basis for the Reynolds equation, is no longer valid. A CFD approach could be used, but since this calculation would have to be repeated in each iteration at the expense of massive computation time, a detailed mass and energy balance becomes more appropriate in the scope of the present work.

The aim of this balance is to estimate the temperature of the inlet section of the bearing land located downstream of this groove (also called the leading edge of the groove). This temperature will be the initial condition to be supplied for the resolution of the energy equation at the fluid domain located downstream of that grove. In the present work this balance takes into account: all major inbound and outbound heat fluxes due to lubricant flow across the boundaries of the groove region; the heat fluxes due to forced convection between the bush body and the inner groove lubricant; the influence of the actual groove dimensions, namely the groove length ratio, a/b; the occurrence of fresh oil backflow (upstream of the groove) and reverse flow (downstream of the groove); the influence of the occurrence of negative feeding flow rate (hot oil reflux) in one of the grooves; the existence of a non-uniform temperature profile at the inlet section (leading edge of the groove). An outline of the heat fluxes crossing the boundaries of the groove region is presented in Fig. 5(a).

But the thermal balance is not sufficient, by itself, to determine the several average temperatures corresponding to the various outward lubricant flows and the inner groove temperature, $\overline{T}_{gr}$. Regardless of the mixing efficiency, it seemed reasonable to assume that the backflow temperature, $\overline{T}_{bkf}$ and the axial flow temperature $\overline{T}_{axial}$ will be similar to $\overline{T}_{gr}$. However, the average leading edge temperature will depend on the degree of mixing

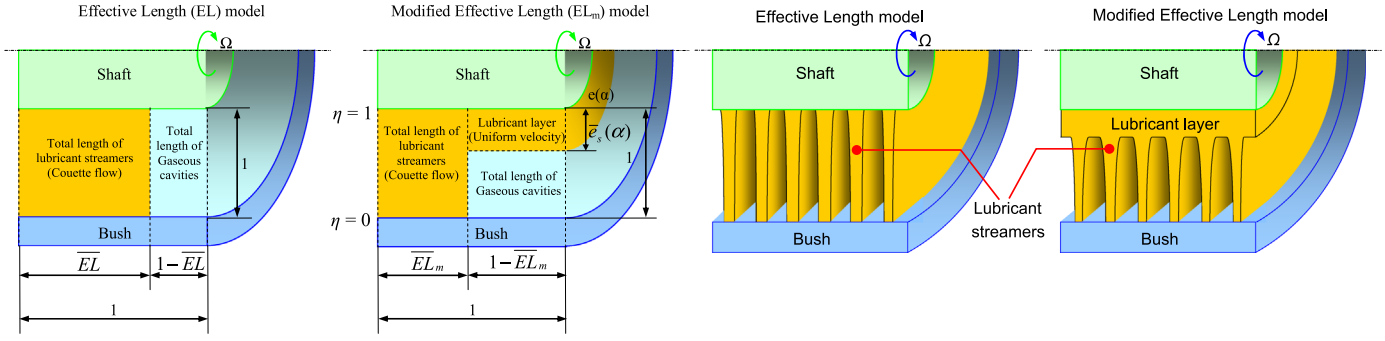

Fig. 4. Outline comparison between the Effective Length and the modified Effective Length thermal models of the ruptured film region proposed in the present work.

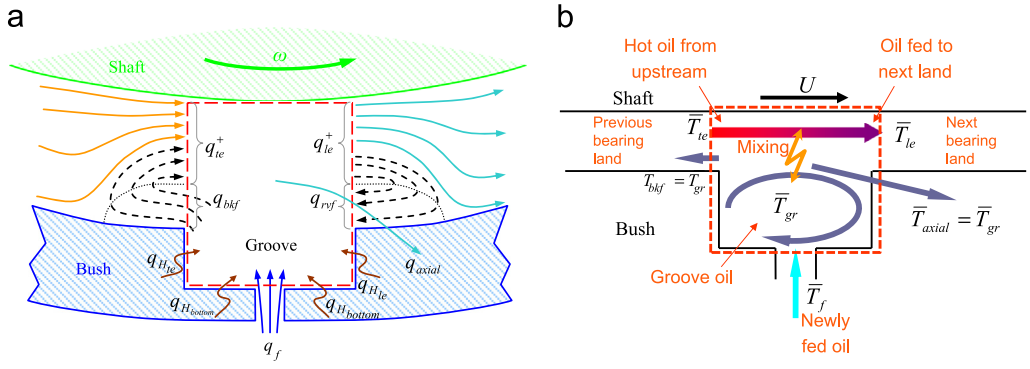

Fig. 5. (a) Heat fluxes across the boundaries of the groove region in the presence of back flow upstream and reverse flow downstream of the groove and (b) Outline of the thermal mixing model within the groove region.

between the hot oil coming from upstream and reaching the trailing edge of the groove at an average temperature $\overline{T}_{te}$ and the inner groove oil at temperature $\overline{T}_{gr}$. An outline of the mixing process is sketched in Fig. 5 (b).

A mixing coefficient, c_{mix} was introduced:

$$\overline{T}_{gr} = c_{mix}\overline{T}_{le} + (1 - c_{mix})\overline{T}_f \tag{10}$$

where c_{mix} may vary between two theoretical limits:

- Perfect mix ($c_{mix}=1$), with the oil reaching the groove from upstream perfectly mixing with the inner groove oil, in which case all four outward temperatures will be virtually identical, that is, $\overline{T}_{gr} = \overline{T}_f$.
- No mixing at all ($c_{mix}=0$), where all recirculated hot oil is re-fed to the next bearing land without the occurrence of any heat exchange with the groove oil, that is, the groove oil will be solely affected by the lubricant feeding temperature and thus, $\overline{T}_{gr} = \overline{T}_f$.

The mixing efficiency within a groove is likely to depend on several factors and is out of the scope of this work. A fixed value of 0.1 has been selected after a brief parametric study. This small mixing coefficient is in agreement with the CFD study of Kosasih and Tieu [36], which concluded that although the flows occurring within the groove interior are highly recirculating, they have almost negligible effects on thermal mixing.

It is now possible to derive the leading edge temperature, $\overline{T}_{le}$, from the thermal balance expressed in Fig. 5:

$$\overline{T}_{le} = \frac{\overline{q}^{+}_{te} + \overline{q}_H + \overline{Q}_f\overline{T}_f + |\overline{q}_{rvf}| - (|\overline{Q}_{axial}| + |\overline{Q}_{bkf}|)(1 - c_{mix})\overline{T}_f}{c_{mix}|\overline{Q}_{axial}| + c_{mix}|\overline{Q}_{bkf}| + \overline{Q}^{+}_{le}} \tag{11}$$

The present thermal approach is 2D, made in the mid-plane of the bearing, and, as already mentioned when describing the assumptions made, several studies have confirmed that in most cases the axial temperature gradients along the bearing length are indeed negligible and what happens at the mid-plane is representative of the whole bearing length. However, if the grooves have a small length, the mid-plane thermal analysis made above should be corrected in order to reflect, on average, the whole bearing length, and not just the grooved length.

With the knowledge of the 3D velocity field it is possible to estimate the average inlet section temperature, $\overline{T}_{is}$, which reflects more accurately the effective temperature of the whole bearing length. This temperature will be calculated from a balance that includes not just the flow rate and the temperature of the lubricant leaving the groove, $\overline{T}_{le}$, but also the flow rate and temperature of the oil flowing at the portion of the bearing length which is not covered by the groove, $\overline{T}_{le\_side}$, as depicted in Fig. 6.

Thus, the energy and mass balances performed to the groove and the dotted control volume depicted in Fig. 6 yields the following expressions:

$$\overline{T}_{is} = \frac{\overline{Q}^{+}_{le}\overline{T}^{+}_{le} + \overline{Q}_{le\_side}\overline{T}_{le\_side}}{\overline{Q}^{+}_{le} + \overline{Q}_{le\_side}} \quad \text{with} \quad \overline{T}_{le\_side} = \frac{\overline{Q}_{te\_side}\overline{T}_{te} + \overline{Q}_{axial}\overline{T}_{axial}}{\overline{Q}_{te\_side} + \overline{Q}_{axial}} \tag{12}$$

2.2.4. Conditions at the interfaces

The conditions set at the various interfaces, as already outlined in Fig. 3, are presented in continuation.

At the shaft-film interface a condition of no net heat flux was imposed. This may be considered as a midterm between situations where the shaft acts a heat sink or a heart source. Also, the shaft surface temperature is considered to be constant, following experimental evidence [31]. These two assumptions are widely accepted and used in the literature [16,37,38].

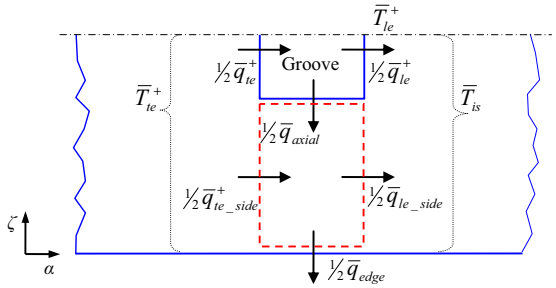

Fig. 6. Outline of the thermal balance carried out to determine the average inlet section temperature, $\overline{T}_{is}$, which incorporates the influence of the groove length ratio, a/b.

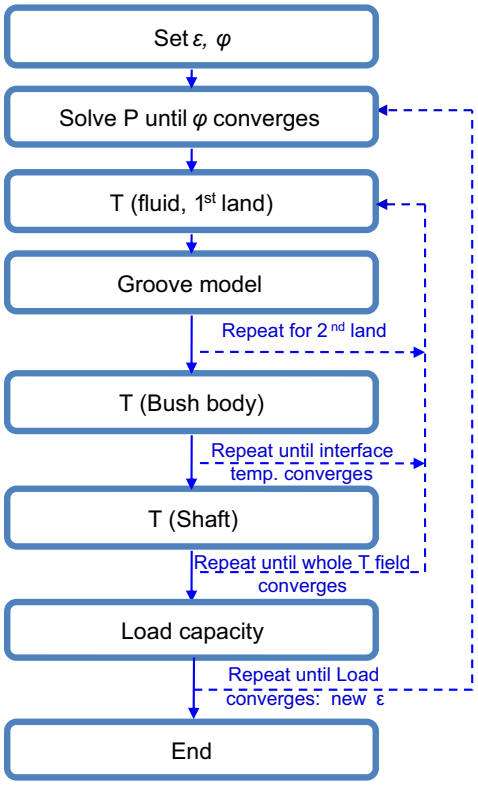

Fig. 7. Outline of the numerical algorithm.

At the bush-film interface, the temperature and heat flux continuity are applied, while natural and forced convection conditions are used at the bush-ambient interface and at the inner groove walls, respectively. It is worth noting that the accounting for convective heat transfer at the groove walls must be done both in the bush body conduction calculation and in the groove thermal balance. Otherwise, a virtual heat source/sink will exist due to this. A higher than usual value of 750 W/m^2 K was chosen for H_{gr}. Such value appears to be in better agreement with the highly recirculating flow found within groove regions [36,39] and indeed this allowed to replicate the strong temperature fade found experimentally in the vicinity of grooves [24].

2.3. Numerical procedure

The theoretical model was implemented using the FORTRAN 90/95 programming language. The global solution algorithm is outlined in Fig. 7.

The selection of the mesh parameters and convergence criteria was based on a comprehensive parametric study in order to obtain a good compromise between accuracy and processing time. The

approach relied on the use of refined meshes in order to detect more subtle phenomena such as reverse flow. 221 Nodes were used in the circumferential direction, 30 in the axial direction (half bearing length) and 35/50 in the radial direction (in the fluid/solid domain, respectively). The two cells in the vicinity of the groove edges were refined by a factor of six after the first few iterations. Taking into account the small randomness found in the results (even at very high eccentricities), along with the small differences found between the results obtained with the final mesh and the finest meshes tested, the present algorithm seems to be particularly robust. The mesh parameter optimization was detailed in [29].

2.4. Model validation

There is a lack of models presenting a thorough validation with experimental data, something which compromises the reliability of the results obtained. Such was tried with the present model. A comparison against the results of Ferron et al. [32], which are extensively used in model validation, can be seen in Fig. 8.

A very good theoretical–experimental correlation is obtained for maximum temperature (T_{max} – Fig. 8a) with differences of around 1 °C, within the error of temperature measurements. The temperature trend is fairly well predicted for both cases except in the region immediately downstream of the groove, as seen in Fig. 8a. This may have happened due to the fact that, while the experimental values were measured at the mid-plane of the bearing, the theoretical approach performs averaged thermal calculations over the whole section. The hydrodynamic pressure profiles displayed in Fig. 8b are within the experimental error margin, the same happening with the estimation of eccentricity ratio. Flow rate (Fig. 8c) has been slightly overestimated.

Fig. 9 presents the predicted temperature profiles against experimental results obtained by the authors [40]. Again, it should be highlighted that the temperature correlation in the region immediately downstream of grooves is not satisfactory since the predicted values are representative of the whole section and not just of the mid-plane, as measured experimentally.

The suitability of the predictions may be better acknowledged by observing the peak temperatures occurring in each one of the bearing lands and also on the shaft surface (see Fig. 10). In fact, seldom has the temperature trend in the ruptured film region of twin groove journal bearings been accurately predicted. The

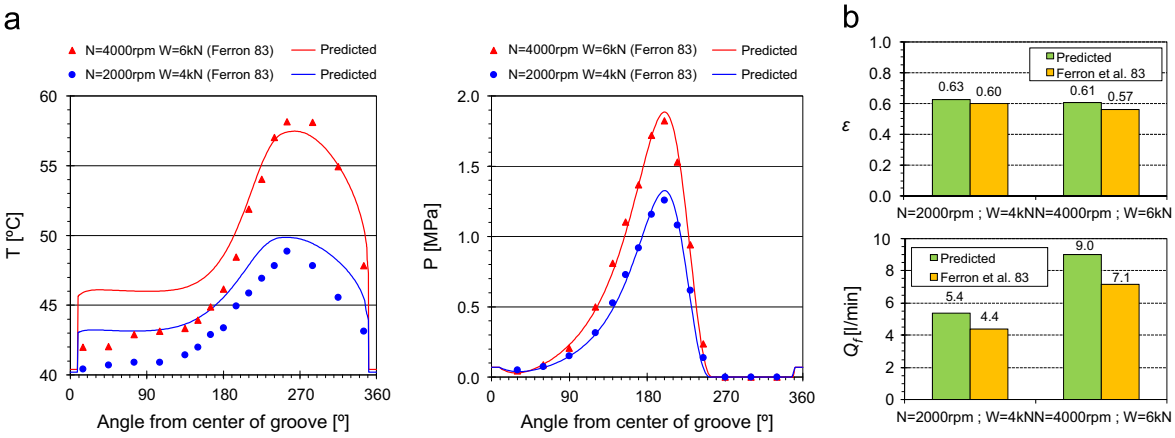

Fig. 8. Comparison between the present analysis and experimental data [32] under two different conditions, for (a) inner bush surface temperature profile (b) pressure profile at the mid-plane of the bearing and (c) eccentricity ratio and flow rate.

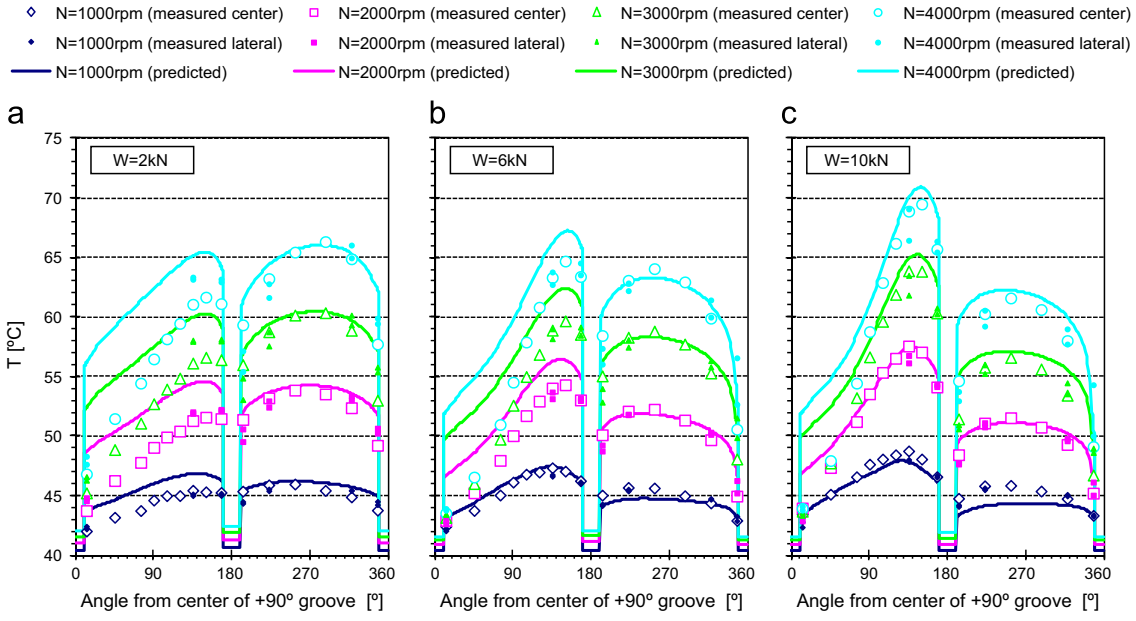

Fig. 9. Comparison between the present analysis and experimental temperature profiles at the mid-plane of the inner bush surface of the bearing for four different shaft speeds and an applied load of (a) 2 kN, (b) 6 kN and (c) 10 kN; (d) Total flow rate (P_f=140 kPa) [40].

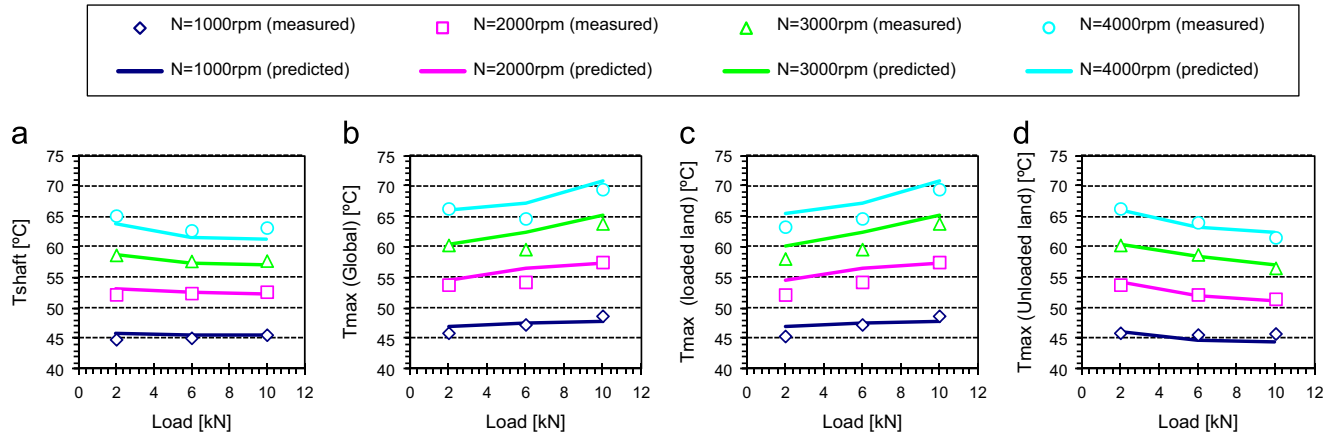

Fig. 10. Comparison between theory and experiment, for several loads and shaft speeds, of (a) Shaft surface temperature, (b) maximum bush temperature, (c) maximum bush temperature at the loaded (lower) land and (d) maximum bush temperature at the unloaded (upper) land of the bearing (P_f=140 kPa); [40].

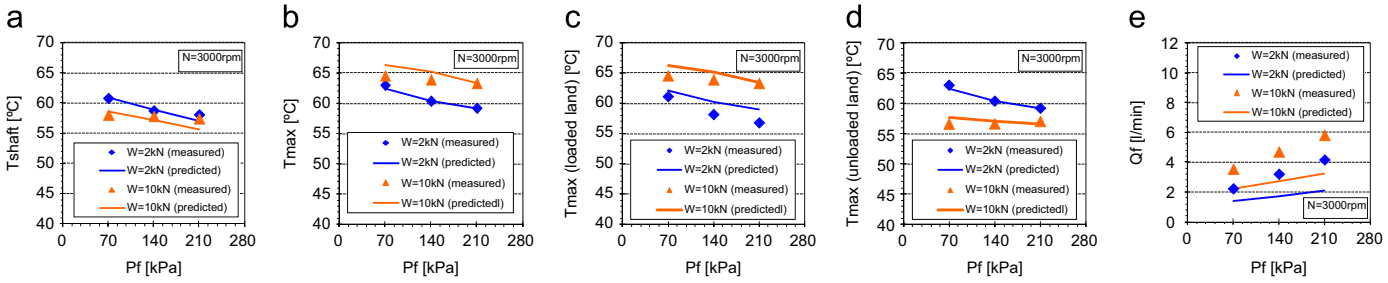

Fig. 11. Comparison between theory and experiment, for several loads and feeding pressures, of (a) Shaft surface temperature, (b) maximum bush temperature, (c) maximum bush temperature at the loaded (lower) land, (d) maximum bush temperature at the unloaded (upper) land of the bearing and (e) flow rate [24].

present model seems to accomplish this rather satisfactorily for the generality of the tests, as seen in Fig. 10.

Fig. 11 depicts the comparison of the predictions of the present analysis against experimental results from another paper by the group [24] in which the same test rig was used for similar operating conditions, but where the feeding pressure varied threefold from 70 to 210 kPa. The same good correlation may be observed (something positive for the present analysis, in the scope of the assessment of feeding conditions), except for the flow rate, which was substantially underestimated.

Unfortunately, the crude underestimation of the flow rate in twin groove journal bearings analyses is a commonly known issue, still unresolved and found in numerous reference works [8,9,11,16] and even popular bearing design tools [41]. This might be linked with the intrinsic limitations in the modeling of flow in grooves located in the midst of the ruptured film region [42] and requires further investigation. Nonetheless, this general underestimation does not seem to decisively affect the maximum temperature of the bush, which has been fairly well predicted in most cases. In fact, it can be seen in the experimental data of Fig. 11 that when the flow rate was doubled (by increasing P_f from 70 to 210 kPa, Fig. 11e) it had an impact of only 1 °C in maximum bush temperature for the high load case (Fig. 11b). In the low load case the measured decrease of T_{max} was somewhat higher (4 °C). So, it seems that for high loads the increase of flow rate only marginally affects T_{max}. Maybe that is why the substantial under-prediction of flow rate still allowed for a good prediction of T_{max}. In the low load case the flow rate differences seemed to affect portions of the temperature profile (namely at the loaded land of the bearing, as already seen in Fig. 9a) but not so much T_{max}.

Therefore, the current model seems apt to be used in the analysis of the performance of single and twin groove hydrodynamic journal bearings with realistic feeding conditions.

3. Analysis of lubricant feeding conditions

In continuation, the lubricant feed conditions such as the lubricant feeding pressure and temperature, the groove length ratio (a/b), the groove width ratio (w/d) and the number of grooves (single/twin) are analyzed for a bearing geometry which is roughly the one used in the test rig of Refs. [24,40]. This analysis aims to assess how these parameters may affect bearing performance and how they can be optimized to achieve a reduction in friction without sacrificing the integrity of the system. The input parameters used in the analysis are presented in Tables 1 and 2, with the default conditions being represented in bold.

3.1. Feeding pressure (P_f)

Feeding pressure (P_f) is one of the feeding parameters which is frequently neglected in modeling as its analysis requires a realistic treatment of groove geometry and a mass conserving algorithm with film rupture and regeneration front estimation. Nonetheless, it affects deeply the thermal behavior of the bearing due to its cooling effect. Also, if the bearing is too starved, contact might occur, while if there is lubricant excess there will be increased power loss.

Fig. 12 shows the effect of P_f on the total flow rate and on the flow rate through each groove, for a broad range of specific loads.

While total flow rate follows a well-known trend with load, the flow rates through each groove show rather dissimilar or even opposite trends. This phenomenon has already been observed experimentally and explained in several of the authors' publications [25–28,43], including the curious phenomenon of negative flow rate occurring at high loads in the +90° groove, the groove which serves the loaded land of the bearing (also called the upstream groove). This means that this groove starts acting as a

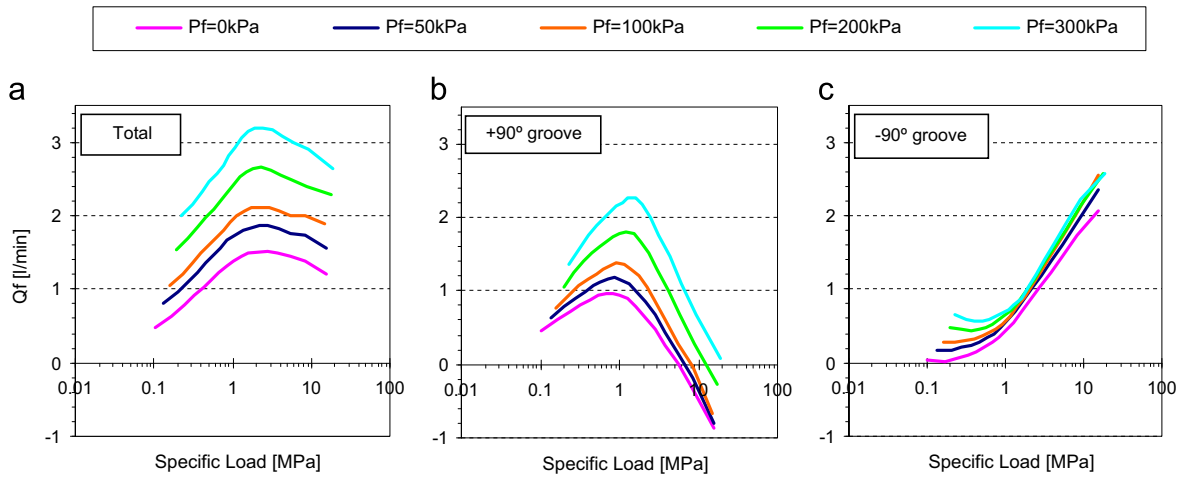

Fig. 12. Influence of specific load and lubricant feeding pressure on (a) total flow rate, (b)+90° groove flow rate and (c) −90° groove flow rate (N=3000 rpm).

lubricant sink instead of a lubricant source for the bearing. This behavior is caused by the excessive closeness between the groove and the strong hydrodynamic pressures, which eventually exceed feeding pressure, reversing pressure gradients and thus the direction of the lubricant flow. This phenomenon occurs under heavily loaded conditions and thus raises the seizure risk. In fact, the lubricant is being retrieved just upstream of the active bearing region, where it would be most needed. And this lubricant starvation might happen inadvertently since the total flow rate (the parameter which is measured in industrial applications, at best) will indicate a seemingly normal feeding flow rate value. Here it can be seen that the increase of P_f plays an important role in preventing this phenomenon as seen in Fig. 12b.

The effect which P_f has on power loss, minimum film thickness (h_{min}) and maximum bush temperature (T_{max}) may be observed in Fig. 13a, b and c, respectively. Indeed, when increasing P_f h_{min} increases, something which is generally positive. However, this is obtained at the expense of an increase in power loss from 9% to 30% for a threefold increase in P_f. This is due to the fact that a higher flow rate of oil will reduce the average oil temperature and thus increase viscosity and viscous drag. Also the full film region will be somewhat broader, and so the viscous drag will further increase.

By looking at Fig. 13c it can be seen that T_{max} is not minimized in the presence of the lowest loads but rather slightly higher values of this parameter. This is due to the fact that lightly loaded bearings typically display a low rate of lubricant leakage/renewal, as observed experimentally [24]. However, it can be observed that an increase in P_f might indeed reduce T_{max} significantly for light load conditions.

Fig. 14 displays the effect which P_f has on the inner bush surface temperature profile for a light, a medium and a heavy load. It can be seen that T_{max} is higher for W_s=0.1 than for W_s=1 MPa under low P_f (100 kPa). Not so when increasing P_f to 300 kPa.

The effect which P_f has on eliminating negative flow rate can be observed in Fig. 14c in the unloaded land of the bearing. Indeed, when P_f=100 kPa it can be seen that the +90° (upstream) groove provides no cooling to the system, that is, no fresh oil is fed to the bearing gap since flow rate through this groove is negative (recall flow rate plot in Fig. 12b). Once increasing P_f from 100 kPa to 200 kPa the groove temperature drops abruptly from 64 °C to 42 °C, a value close to the feeding temperature (40 °C). This indicates that the flow rate has started to be positive.

3.2. Feeding temperature (T_f)

Lubricant viscosity, which strongly depends on temperature, is the parameter responsible for hydrodynamic pressure generation within the fluid. Therefore, the variation of T_f is likely to exert a strong influence not only on the temperature field, the power loss and the flow patterns, but also on minimum film thickness and ultimately on the load carrying capacity of the bearing.

On one hand, if T_f is too low, the viscosity of the lubricant will be high and an excessive power loss will exist. On the other hand, if T_f is too high there will be no sufficient load carrying capacity, with risk of contact. Besides, the thermal crowning of surfaces due to thermal distortion will further raise the risk of seizure.

Fig. 15 displays the same flow rate data but now as a function of two different variables, specific load and eccentricity ratio. Within the lower range of specific loads (below 2 MPa) the flow rate at the +90° groove increases when T_f rises, indicating the fall on viscosity suffered by the hotter lubricant. However, the opposite occurs for higher specific load values. The reason for this lies in the rise in eccentricity ratio which is much more pronounced for higher loads. In fact, when analyzing this same data, but seen as a function of eccentricity ratio (see Fig. 15d, e and f) it is apparent that this latter parameter plays a decisive role in flow rates. For instance, negative flow rate seems to start occurring for an eccentricity ratio around 0.9 irrespective of the value of T_f. This corresponds to between 8 and 10 MPa specific loads, depending on T_f.

The increase of eccentricity (or the decrease in minimum film thickness) with increasing T_f may be observed in Fig. 16a, while the effect of T_f on the maximum temperature and shaft surface temperature as well as power loss is displayed in Fig. 16b and c, respectively. As expected, the viscosity reduction caused by the increase in T_f with temperature yielded a decrease of the viscous dissipation and, therefore, of the power loss. For instance, a 30% reduction in power loss may be obtained when increasing T_f from 30 °C to 60 °C, for a specific load around 1 MPa.

A comparison between the temperature profiles for T_f of 30 °C and 60 °C is presented in Fig. 17 for a wide range of specific loads.

In accordance with the experimental observations [24,26], the increase in T_{max} is always much less than the corresponding increase in T_f: in this case, a 30 °C increase in T_f yielded increases of 7 °C for the lowest load case (W_s=0.1 MPa) and 15 °C for the highest (W_s=10 MPa). Another interesting fact is that the increase of T_f triggered the appearance of the hot oil reflux phenomenon in the test with W_s=8 MPa, as seen in Fig. 17b.

3.3. Groove length ratio (a/b)

Despite the present thermal model being 2D (performed in the bearing mid-plane only), the pressure and flow calculations are

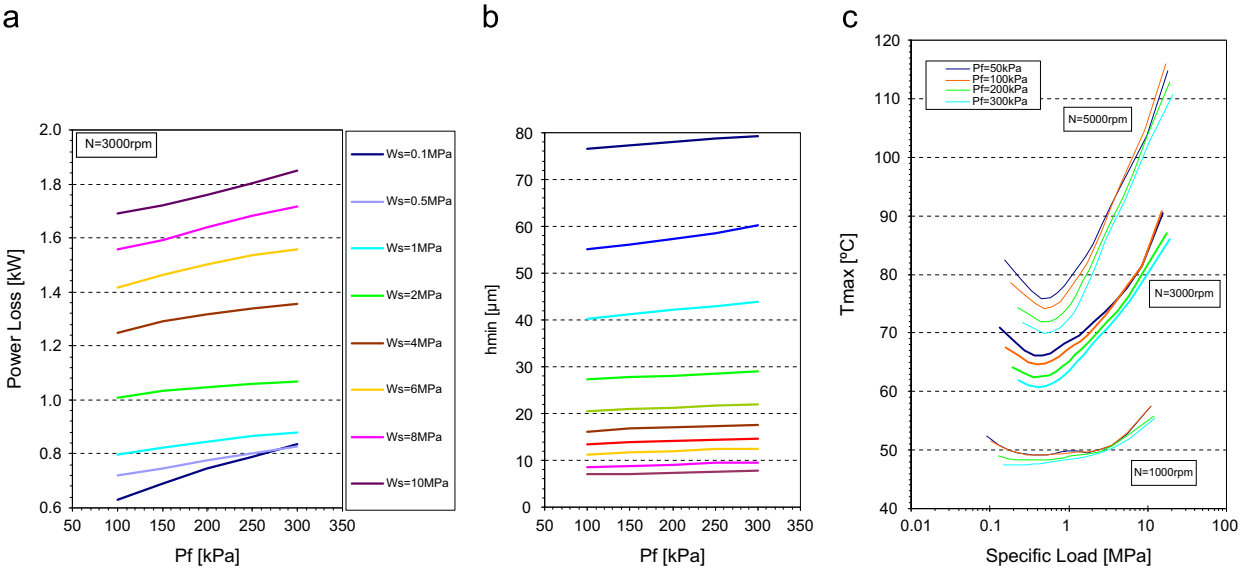

Fig. 13. Temperature profiles at the midplane of the inner bush surface for several feeding pressures and (a) W_s=0.1 MPa, (b) W_s=1 MPa and (c) W_s=8 MPa. (N=3000 rpm).

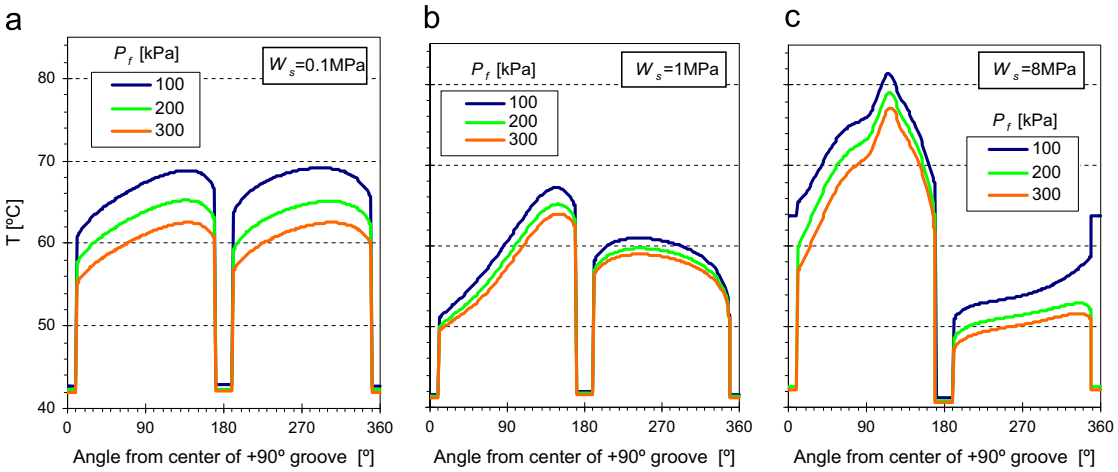

Fig. 14. Influence of feeding pressure on (a) minimum film thickness and (b) power loss.

performed in the whole 3D fluid domain and the thermal balances of the groove regions (the places where axial temperature differences might be significant) have incorporated the influence of a/b, as noted when describing the model.

The hydrodynamic pressure fields obtained for two bearings with dissimilar a/b ratios (0.3 and 0.875), along with the delimitation of the regions of full and ruptured film are presented in Fig. 18a and b, respectively. The two different groove geometries can be distinguished by observing their constant pressure plateaus ($P=P_f$) in groove regions. In the vicinity of the $+90^\circ$ groove and in the region downstream of it, it can be seen that there are some differences between the pressure fields obtained for the two cases: in the case of the large grooved bearing, there is hydrodynamic pressure generation immediately downstream of this groove extending to the whole axial length of the bearing. On the contrary, in the case of the small grooved bearing, the pressure build-up zone only extends to the whole bearing length further downstream.

The lower extension of the full film region caused by decreasing groove length is translated into a lower carrying capacity, that is, a higher eccentricity for a given applied load, as confirmed by inspecting the eccentricity ratio plot in Fig. 19a. The effect of a/b upon the flow rates can be observed in Fig. 19b. As expected, the total flow rate increases with the increase of a/b since the edges of the groove are farther from the exterior and so there is increased resistance to oil leakage. In this case, total flow rate more than doubled when increasing a/b from 0.3 to 0.875. If lower a/b values tend to decrease flow rate, then it is natural that T_{max} and T_{shaft} should increase due to the lower cooling power provided by the lubricant flux, as confirmed in Fig. 19c.

Fig. 19d shows a positive effect of decreasing groove length, which is the substantial cut in the power loss obtained (around 35% in the whole load range) when decreasing a/b from the highest to the lowest value tested. It should be noted, however, that localized lubricant feed might originate dry regions in the bearing gap (namely close to edges) and promote uneven thermal distortion. If these phenomena are combined with some misalignment, localized contact might occur. So, reducing groove length in order to obtain reduced power loss is a solution which should be carefully assessed.

3.4. Groove width ratio (w/d)

The increase of the circumferential extension of groove, also called the groove width, w, will affect bearing performance in various

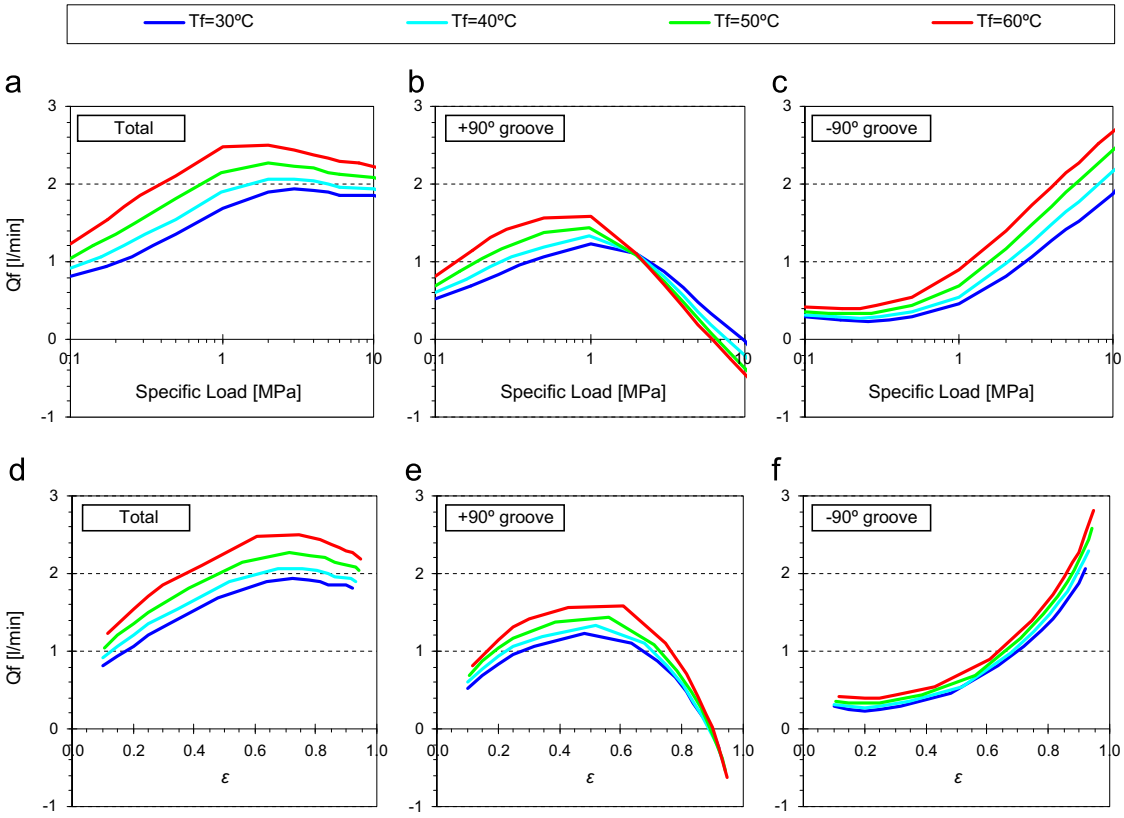

Fig. 15. Influence of specific load/eccentricity and lubricant feeding pressure on (a)/(d) total flow rate, (b)/(e)+90° groove flow rate and (c)/(f) −90° groove flow rate.

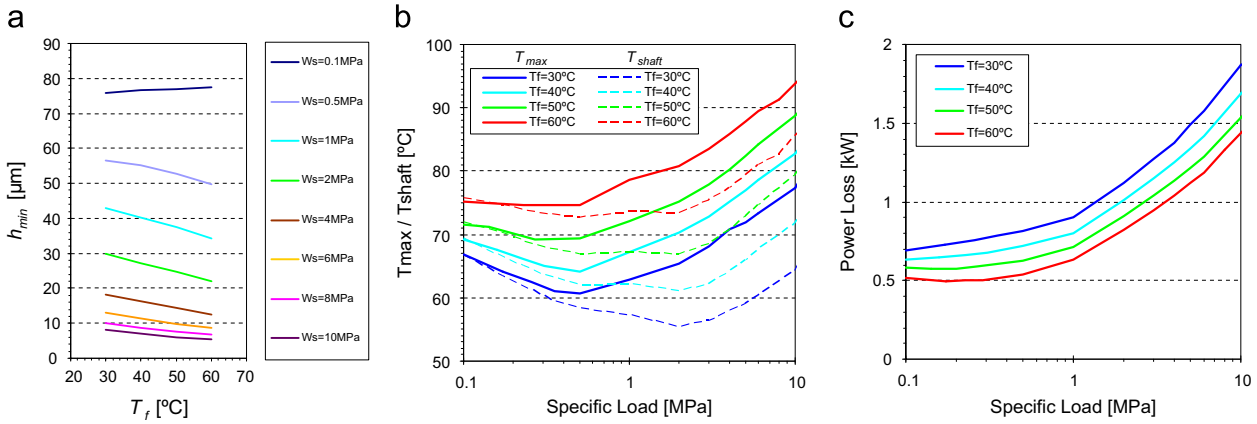

Fig. 16. (a) Influence of feeding temperature on (a) minimum film thickness, (b) maximum bush temperature and shaft surface temperature and (c) power loss as a function of specific load (N=3000 rpm).

ways as it reduces the extension of the bush lands and therefore, there will be a loss of load supporting area and load capacity, especially if the grooves are close to the pressure build-up region.

The total and partial flow rates in each groove are presented in Fig. 20a for the two w/d values tested. Curiously, the total flow rate was not significantly affected by the changes in w/d. However, when increasing w/d, the flow rate at the $+90^\circ$ groove suffered a strong decrease, especially for specific loads higher than 0.3 MPa, while the opposite happened in the -90° groove. As a consequence, the critical W_s for the occurrence of hot oil reflux was lowered from around 8 MPa to about 4 MPa when increasing w/d.

Fig. 20b–d shows the influence of w in the inner bush surface temperature profiles of lightly to heavily loaded bearings. On one hand, the general lowering of the temperature level is apparent in these plots and also in Fig. 21a, which depicts T_{max} and T_{shaft}. Curiously, and unlike what happens with other feeding conditions, this temperature decrease happens simultaneously with a reduction in power loss despite the increase of the average lubricant viscosity due to temperature lowering. This means that the reduction in power loss should be mainly associated to the reduction of the circumferential extension of the bush lands. Under those conditions, viscous drag will occur in a smaller angular extension, thus reducing the overall drag.

The reduction of the global temperature level should also be due to a stronger cooling effect of the groove oil by convective heat transfer over a broader groove surface (recall that convective heat transfer inside the groove has been included in the modeling).

Of course, there should be limits to the beneficial effect of increasing w, namely because the area for load support will be reduced when w is increased. Also, the oil reflux phenomenon will be amplified with the pressure build-up zone getting closer to grooves.

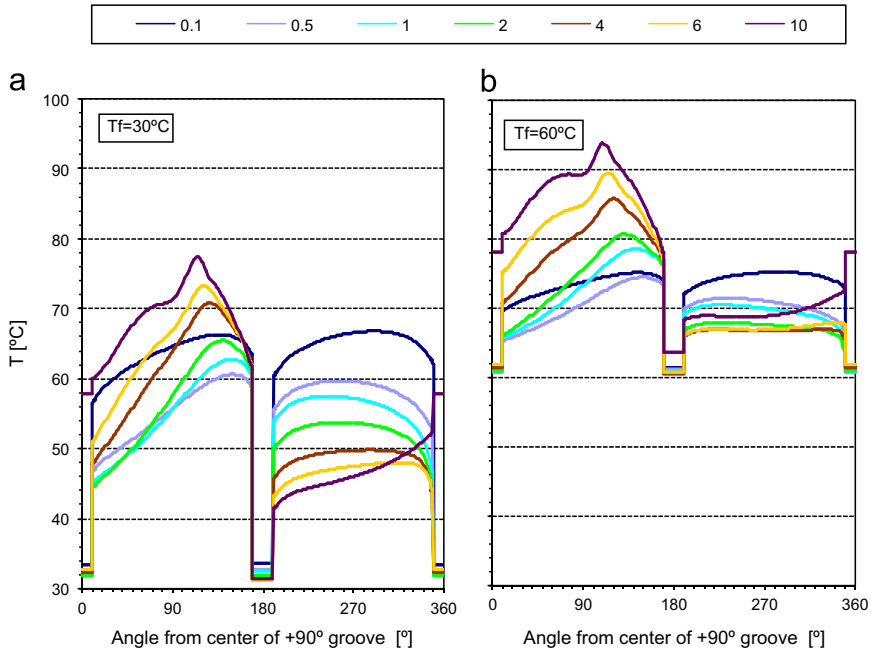

Fig. 17. Temperature profile at the midplane of the inner bush surface for several specific loads and (a) T_f=30° and (b) T_f=60 °C.

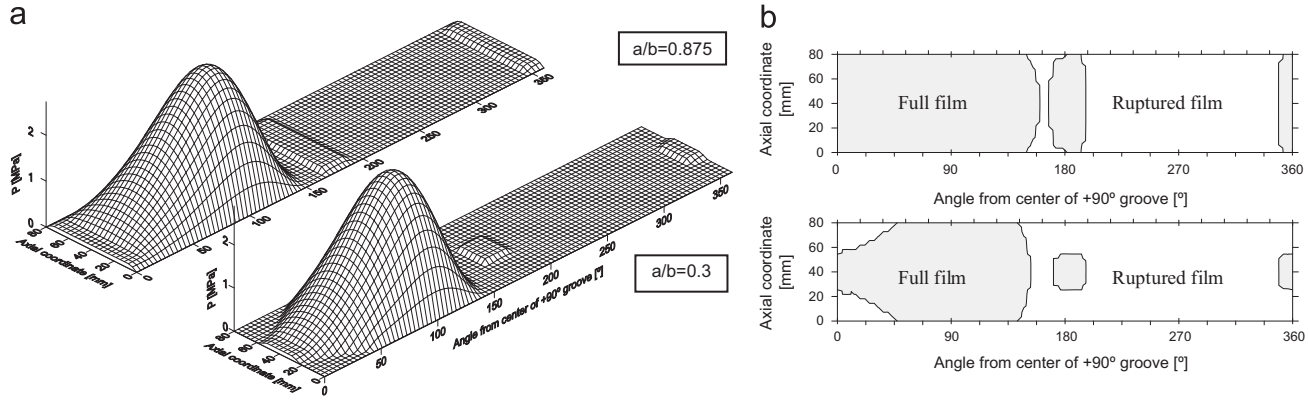

Fig. 18. Influence of groove length ratio on (a) the hydrodynamic pressure field and (b) extension of full film and ruptured film regions (W_s=1.1 MPa).

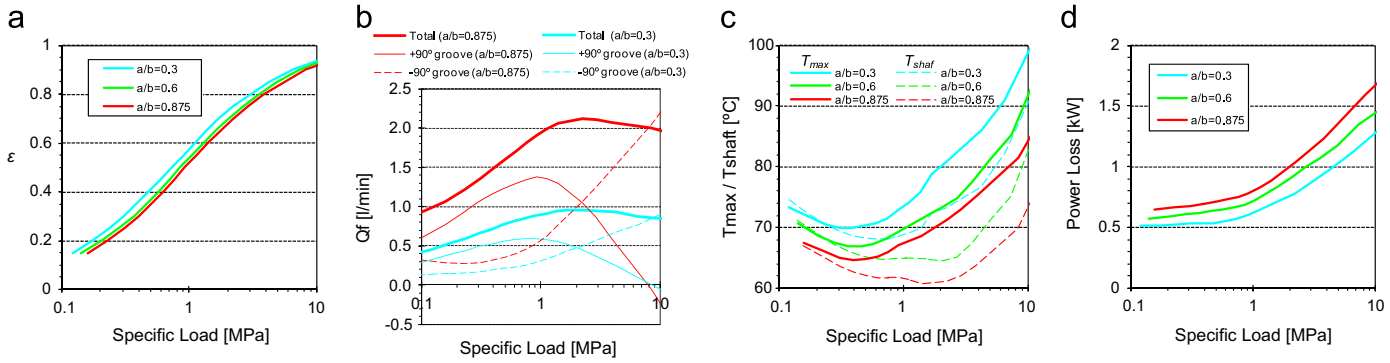

Fig. 19. Influence of the groove length ratio on (a) the global and partial flow rates in each groove, (b) shaft temperature and maximum bush temperature and (c) power loss, for varying specific load.

3.5. *Number of grooves*

The comparison of the performance of single (at +90° to the load line) and twin groove (±90°) hydrodynamic journal bearings for the same operating conditions has seldom been made either theoretically or experimentally. The common sense perception that a twin groove bearing will operate at a lower temperature and with a more efficient lubrication than the single groove one still needs to be confirmed. Recently the authors published an experimental work focusing on this issue [27].

Fig. 22a displays the flow rates corresponding to both cases. It is interesting to acknowledge that the total flow rate is nearly the same for the two bearings along the whole load range, something which was already observed in the experimental work. This means

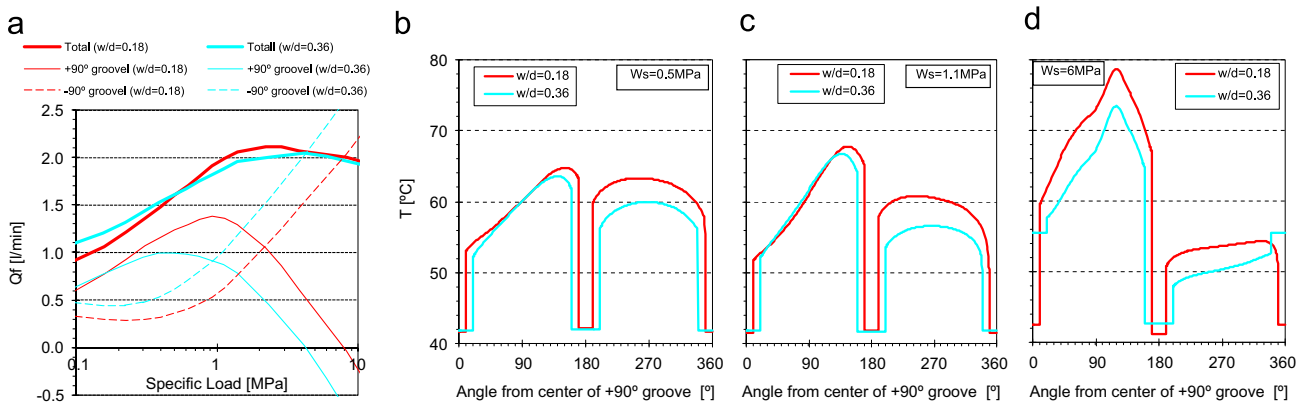

Fig. 20. Influence of groove width ratio on the temperature profiles at the midplane of the inner bush surface for (a) W_s=0.5 MPa, (b) W_s=1.1 MPa and (c) W_s=6 MPa.

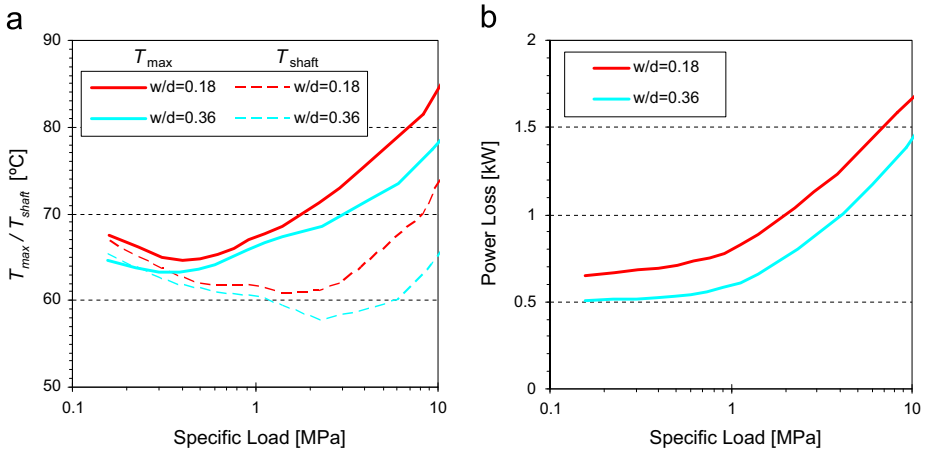

Fig. 21. Influence of groove width ratio on (a) maximum bush and shaft surface temperature and (b) on power loss.

that a redistribution of the same flow rate towards two grooves happens instead of an increase of total flow rate.

The effect of groove number on shaft locus may be seen in Fig. 22b, with the attitude angle of the single groove case being higher than that of the twin groove one, especially for low eccentricities. This is a well known characteristic of single groove bearings: the resulting force caused by the hydrostatic pressure in the groove region (the feeding pressure), is not being canceled by a symmetrical force on the opposite side of the bearing, as it would happen with the twin groove case. Therefore, in the presence of a single groove bearing, the shaft centreline tends to move away from the $+90^\circ$ groove towards the opposite side, thus increasing the attitude angle. Differences in eccentricity for a given load are more easily apprehended in a separate chart as a function of specific load, as seen in Fig. 22c. According to this plot it seems that twin groove bearings operate at a lower eccentricity, thus farther from contact than single groove ones. The reason for this seems to be that the temperature level of twin groove bearings is lower than that of single groove bearings, thus operating with higher oil viscosities, as seen further ahead.

Fig. 23 displays the temperature field in the mid-plane of the bearing for both groove configurations and a specific load of 3.9 MPa. Fig. 23a shows the inner bush surface temperature only, while Fig. 23b pertains the whole fluid (lubricant) and solid (bush) domains. The differences (namely, 12 °C in T_{max}) are quite significant. This can be better understood by taking into account the following chain of effects: the less efficient cooling of the single groove configuration causes a higher fluid temperature, which in turn causes a loss in lubricant viscosity, which originates higher eccentricity, thus aggravating the temperature excess.

This dramatic difference of the temperature levels of the two groove configurations with increasing load can be further observed in Fig. 24a, which displays the evolution of T_{max} and T_{shaft} with W_s. Here it can be seen that the number of grooves also affects significantly T_{shaft}, with differences in T_{max} and T_{shaft} being as high as 25 °C and 30 °C, respectively.

These factors also deserve to be analyzed as a function of eccentricity ratio (b). This can help isolating the temperature effects of the two factors which were pointed out as being responsible for the temperature rising (ineffective cooling and eccentricity increase). In fact, if eccentricity is kept constant, the differences in T_{max} and T_{shaft} are exclusively linked with the cooling efficiency. It can be seen that even canceling the effect of eccentricity variation on temperature there are still significant differences between the two cases (as much as 15 and 20 °C for T_{max} and T_{shaft}, respectively).

The number of grooves also seems to significantly affect the power loss, as seen in Fig. 24c. The reduction in this parameter, as high as 25% when eliminating the -90° groove, seems to be associated to the loss of viscosity (and therefore, of heat generation by viscous dissipation) suffered by the hotter oil.

As a concluding remark, it is worth noting that the results just presented seem to indicate that the addition of the -90° groove causes the decrease of temperature level and eccentricity especially for high loads, at the expense of a higher power loss. However, some caution should be taken with the generalization of these results. In fact, it has been observed before that the present model tends to over-predict the $+90^\circ$ groove flow rate in the high eccentricity range for the case of the twin groove bearing. This over-estimation might be affecting significantly the predictions in some cases: if in reality the $+90^\circ$ groove flow rate is much

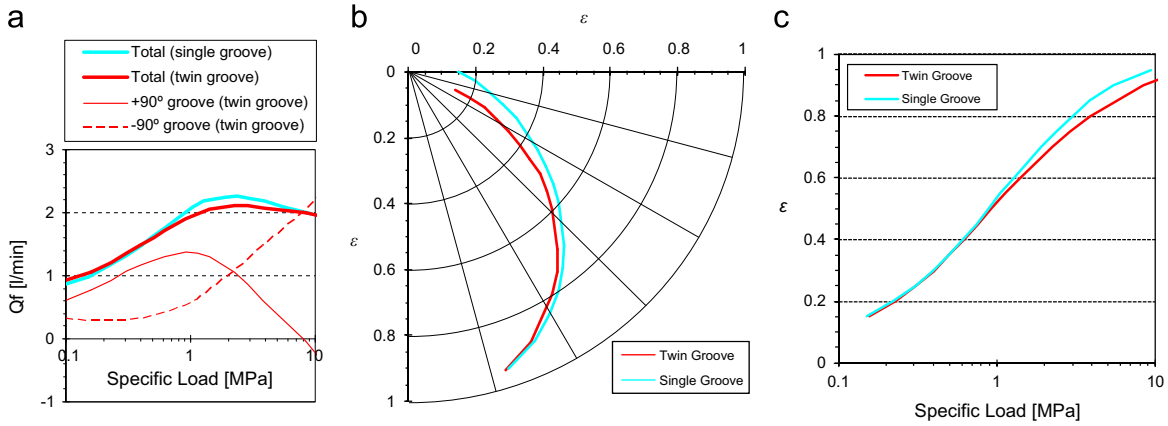

Fig. 22. Influence of the number of grooves on (a) the lubricant flow rates and (b) on shaft locus and (c) on eccentricity ratio.

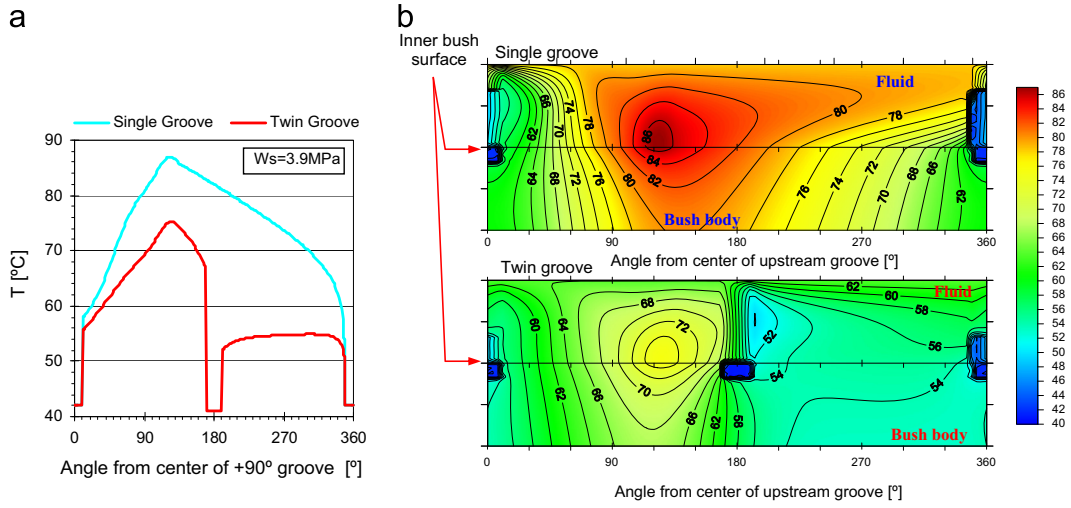

Fig. 23. Influence of the number of grooves on (a) the temperature profile at the midplane of the inner bush surface and (b) the midplane temperature field of the fluid domain and of the bush body domain (W_s=3.9 MPa).

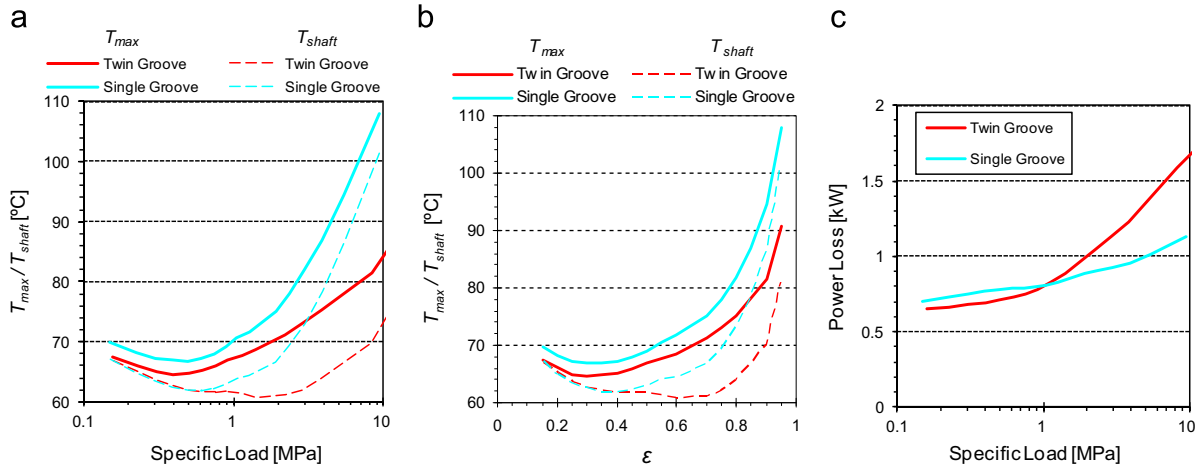

Fig. 24. Influence of the number of grooves on the maximum bush temperature and the shaft surface temperature as a function of (a) specific load and (b) eccentricity ratio. (c) Influence of the number of grooves in power loss.

smaller than predicted, starvation problems might start appearing and become dominant.

The overestimation of the $+90^{\circ}$ groove flow rate is also the reason why the model also tends to over-predict the critical load at which hot oil reflux problems start occurring. In the case studied, this phenomenon was predicted to occur for specific loads above 8 MPa (Fig. 22a). This problem, which is deleterious for bearing performance, namely for eccentricity, appears only in multi groove bearings and has been barely detected in the analysis for these conditions.

Therefore, it is possible that in some situations the oil starvation caused by the splitting of the flow by two grooves instead of

one might become a critical effect, making the twin groove bearing a poorer choice than the single groove bearing. In fact, this seems to be the case with the experimental results presented by the authors in [25,26]. The incorporation of a 3D thermal analysis, along with a more realistic estimation of the thermal and mechanical deformations of the bodies might enable a better prediction of bearing performance in such cases.

4. Conclusions

A Thermohydrodynamic (THD) model for the analysis of hydrodynamic journal bearings with realistic lubricant feed conditions has been proposed and used to assess the role of lubricant feeding conditions on the performance improvement and friction reduction of hydrodynamic journal bearings.

The model is based on the simultaneous solution of the Generalized Reynolds Equation through a mass conserving algorithm and the Energy Equation within the fluid domain, as well as the Laplace equation within the bush body domain.

Care was taken in order to realistically incorporate lubricant feeding conditions into the analysis: the real dimensions of the grooves were considered in pressure and flow calculations. Models for the ruptured film region and the lubricant mixing at the grooves were derived, while a simplified thermo-elastic model was deployed. A thorough validation of the theoretical model was successfully performed and the robustness of the model for a wide range of input conditions was confirmed.

The main factors which can affect the lubricant feeding – feeding pressure and temperature, groove length ratio, groove width ratio and number of grooves (single/twin) were analyzed for a broad range of specific loads, extended well beyond the range of practical applications. In general, the same trends and tendencies which are experimentally observed were predicted by the model. Despite the limitations pointed out in the validation, the results obtained appear to be globally coherent, physically plausible, and with small randomness.

For the conditions tested, the following conclusions may be drawn:

- The feeding pressure proved to be a critical factor in reducing the temperature level of the bearing and in preventing the occurrence of hot oil reflux (negative flow rate in a groove), even if it was at the expense of a higher power loss.
- The increase of the lubricant feeding temperature proved to be beneficial under low loads (it decreased power loss) but especially dangerous under high loads as it strongly increases the eccentricity, T_{max}, P_{max}, and the thermal and mechanical distortions, while lowering the critical load for which hot oil reflux starts occurring.
- The use of smaller length grooves (lower a/b) yielded decreases in power loss around 35%, but at the expense of a less efficient bearing cooling, a smaller extension of complete lubricant film and thus a lower load carrying capacity. If excessive, the narrower range of the lubricant film, combined with the stronger thermal crowning of surfaces due to cooling asymmetries might inclusively cause local contact.
- The increase of w/d induced a decrease in power loss and maximum bush temperature without a significant decrease in load carrying capacity. However, the critical load for which hot oil reflux starts occurring was lowered.
- When comparing single groove ($+90^\circ$ to the load line) and twin groove ($\pm 90^\circ$ to the load line) bearings it was found that the addition of the -90° groove caused a decrease in the temperature level and in eccentricity, especially in the higher load range. The negative effects of adding an extra groove were the increase in power loss and the appearance of hot oil reflux for high eccentricities.

It is true that the present study was performed for a specific (but fairly wide) range of geometries and operating conditions and so a generalization of the aforementioned conclusions should not be lightly taken. Nevertheless, they provide valuable general trends for the role of lubricant feeding conditions in journal bearing performance. It may be stated with confidence that the lubricant feeding conditions may often play a vital role in the performance of hydrodynamic journal bearings and therefore should not be neglected in bearing analyses. A careful tuning of the feeding configuration (geometrical shape, number of grooves, pressure and temperature of supply oil) can result in substantial energy savings and improved operating safety, namely by decreasing working eccentricity and maximum bush temperature and optimized lubricant flow rate. Truly, in some cases the feeding conditions might even dictate the occurrence or the avoidance of bearing damage in ways that conventional bearing design tools are not able to anticipate due to their oversimplified treatment of feeding parameters.

Acknowledgments

Francisco P. Brito benefited from a research Grant in Project POCTI/EME/39202/2001 funded by FCT/EU-FEDER, Ph.D. Grant SFRH/BD/22278/2005 – MCTES-FCT/POPH-QREN, and currently benefits from a Postdoctoral Grant SFRH/BPD/89553/2012 supported by MCTES-FCT/POPH-QREN.

References

[1] Chun S, Lalas D. Parametric study of inlet oil temperature of a half-circumferential grooved journal bearing. STLE Tribol Trans 1992;35:213–24.
[2] Bou Said B. La lubrification a basse pression par le méthode des éléments finis. Application aux paliers, Thèse de doctorat. France: INSA de Lyon; 1985.
[3] Boncompain R, Fillon M, Frêne J. Analysis of thermal effects in hydrodynamic bearings. ASME J Tribol 1986;108:219–24.
[4] Knight JD, Ghadimi P. Effects of modified Effective length models of the rupture zone on the analysis of a fluid journal bearings. STLE Tribol Trans 1992;35:29–36.
[5] Rajalingham C, Prabhu BS. The influence of variation of viscosity with temperature on the steady state characteristics of journal bearings – simple analysis. Tribol Int 1987;20(5):261–6.
[6] Pierre I, Fillon M. Influence of geometric parameters and operating conditions on the thermohydrodynamic behavior of plain journal bearings. Proc Inst Mech Eng, Part J, J Eng Tribol 2000;214:445–57.
[7] Knight JD, Barret L, Cronan RD. The effects of supply pressure on operating characteristics of two-axial groove bearings. STLE Tribol Trans 1985;28:336–42.
[8] Gethin DT, El-Deihi MKI. Thermal behavior of a twin axial groove bearing under varying loading direction. Proc. ImechE, Part C 1990;204:77–90.
[9] El-Deihi MKI, Gethin DT. A thermohydrodynamic analysis of a twin axial groove bearing under different loading directions and comparison with experiment. ASME J Tribol 1992;114:304–10.
[10] Dowson D, Taylor CM, Miranda AS. The prediction of liquid film journal bearing performance with a consideration of lubricant film reformation, Part I and II. Proc. ImechE 1985;119(C2):95–102 (102–111).
[11] Claro JCP, Miranda AS. Analysis of hydrodynamic journal bearings considering lubricant supply conditions. Proc Inst Mech Eng Part C 1993;207:93–101.
[12] Elrod HG. A cavitation algorithm. ASME J Lubr Technol 1981;103(3):350–4.
[13] Costa L, Miranda AS, Fillon M, JCP. Claro. An analysis of the influence of oil supply conditions on the Thermohydrodynamic performance of a single groove journal bearing. Proc Inst Mech Eng, Part J: J Eng Tribol 2003;217:133–44.
[14] Costa L, Fillon M, Miranda AS, JCP. Claro. An experimental investigation of the effect of groove location and supply pressure on the THD performance of a steadily loaded journal bearing. ASME J Tribol 2003;122:227–32.
[15] Ma MT, Taylor CM. Effects of oil temperature on the performance of an elliptical bearing. In: Proceedings of the 21st Leeds-Lyon symposium on tribology, 1994. Tribology series, vol. 30. Elsevier; 1995. p. 143–51.
[16] Ma MT, Taylor CM. A theoretical and experimental study of thermal effects in a plain circular steadily loaded journal bearing. IMechE Seminar: Plain Bearings – Energy Efficiency and Design. London: Mech. Engs. Publications Ltd.; 1992.
[17] Ma MT, Taylor CM. Prediction of temperature fade in cavitation region of two-lobe journal bearings. Proc ImechE 1994;208:133–9.

[18] Vijayaraghavan D. An efficient numerical procedure for Thermohydrodynamic analysis of cavitating bearings. ASME J Tribol 1996;118:555–63.
[19] Vijayaraghavan D, Keith Jr TG, Brewe DE. Effect of lubricant supply starvation on the thermohydrodynamic performance of a journal bearing. Tribol Trans 1996;39:645–53.
[20] Keogh PS, Khonsari MM. Influence of inlet conditions on the thermohydrodynamic state of a fully circumferentially grooved journal bearing. ASME J Tribol 2001;123:525–32.
[21] Tonnesen J, Hansen PK. Some experiments on the steady state characteristics of a cylindrical fluid film bearing considering thermal effects. ASME J Lubr Technol 1981;103:107–14.
[22] Lund JW, Tonnesen J. An approximate analysis of the temperature conditions in a journal bearing. Part II. Appl ASME J Tribol 1984;106(2):237–45.
[23] Fitzgerald MK, Neal PB. Temperature distributions and heat transfer in journal bearings. ASME J Tribol 1992;114:122–30.
[24] Brito FP, Bouyer J, Fillon M, Miranda AS. Experimental investigation of the influence of supply temperature and supply pressure on the performance of a two axial groove hydrodynamic journal bearing. ASME J Tribol 2007;129 (2007):98–105.
[25] Brito FP, Miranda AS, Claro JCP, Fillon M. The role of each groove on the behavior of twin axial groove journal bearings. In: Proceedings of IBERTRIB – Congreso Ibérico de Tribología, Escuela de Ingenieros, Bilbau, CD-ROM; June 20–21, 2007.
[26] Brito FP, Miranda AS, Claro JCP, Fillon M. The role of lubricant supply temperature on the performance of twin groove journal bearings: an experimental study. Int J Surface Sci Eng 2011;5(4):286–99, http://dx.doi.org/10.1504/IJSURFSE.2011.044278 (Inderscience Publishers).
[27] Brito FP, Miranda AS, Claro JCP, Fillon M. Experimental comparison of the performance of a journal bearing with a single and a twin axial groove configuration. Tribol Int, 54; 2012; 1–8 (Elsevier).
[28] Arab Solghar A, Brito FP, Claro JCP, Nassab AG. An experimental study of the influence of loading direction on the thermohydrodynamic behavior of twin axial groove journal bearing. Proc Inst Mech Eng Part J: J Eng Tribol 2011;225 (5):245–54.
[29] Brito FP. Thermohydrodynamic performance of twin groove journal bearings considering realistic lubricant supply conditions: an experimental and theoretical study [Ph.D. thesis]. Guimarães, Portugal: School of Engineering, Universidade do Minho; 2009. Available from: ⟨http://repositorium.sdum.uminho.pt/handle/1822/9884⟩.
[30] Pinkus O. Thermal aspects of fluid film tribology. New York: ASME Press; 1990.
[31] Dowson D, Hudson J, Hunter B, March C. An experimental investigation of the thermal equilibrium of steadily loaded journal bearings. Proc Inst Mech Eng 1966-67;101(Pt 3B):70–80.
[32] Ferron J, Frêne J, Boncompain R. A study of the Thermohydrodynamic performance of a plain journal bearing. Comparison between theory and experiments. ASME J Lubr Technol 1983;105:422–8.
[33] Pierre I, Fillon M. Validity limit of the two-dimensional thermohydrodynamic analysis of plain journal bearings. In: Proceedings of the International Tribology Conference, ITC 2000, vol. III. Nagasaki, Japan: Japanese Society of Tribologists; 29 October–2 November, 2000. p. 1555–60.
[34] Knight JD, Ghadimi P. Analysis and observation of cavities in a journal bearing considering 1flow continuity. STLE Tribol Trans 2001;44:88–96.
[35] Heshmat H. The mechanism of cavitation in hydrodynamic lubrication. Tribol Trans 1991;34(2):177–86.
[36] Kosasih PB, Tieu AK. An investigation into the thermal mixing in journal bearings. Proc Inst Mech Eng Part J: J. Eng Tribol 2004;218:379–89.
[37] Pierre I, Bouyer J, Fillon M. Thermohydrodynamic behavior of misaligned plain journal bearings: theoretical and experimental approaches. Tribol Trans 2004;47(4):594–604.
[38] Jang JY, Khonsari MM. Design of bearings on the basis of thermohydrodynamic analysis. Proc Inst Mech Eng Part J: J. Eng Tribol 2004;218:355–63.
[39] Jeddi L, El Khlifi M, Bonneau D. Thermohydrodynamic analysis for a hydrodynamic journal bearing groove;2005. p. 263–74.
[40] Brito FP, Bouyer J, Fillon M, Miranda AS. Experimental investigation on the thermal behavior and performance characteristics of a twin axial groove journal bearing as a function of applied load and rotational speed. In: Proceedings of the 5th international conference on mechanics and materials in design – M2D′2006, symposium on wear and lubrication in design. CD-ROM. Porto: FEUP; 24–26 July, 2006. ISBN ⟨972-8826-10-9⟩.
[41] ESDU item no. 84031. Calculation methods for steadily loaded axial groove hydrodynamic journal bearings. London: Engineering Sciences Data Unit (ESDU) International Plc.; 1984.
[42] Groper M, Etsion I. Reverse flow as a possible mechanism for cavitation pressure build-up in a submerged journal bearing. ASME J Tribol 2002;124:320–6.
[43] Brito FP, Miranda AS, Claro JCP, Teixeira JC, Costa L, Fillon M. 2012. On the occurrence of negative groove flow rate in twin groove hydrodynamic journal bearings. In: Proceedings of the 15th international conference on experimental mechanics (ICEM15). Porto, Portugal: FEUP; 22–27 July, 2012. p. 875–6. ISBN ⟨978-972-8826-25-3⟩ (Extended Abstract).